Available online at www.sciencedirect.com
ScienceDirect
Agricultural and Forest Meteorology 145 (2007) 1–21
AGRICULTURAL AND FOREST METEOROLOGY
www.elsevier.com/locate/agrformet

CO_2 transport over complex terrain

Jielun Sun [a,*], Sean P. Burns [a], Anthony C. Delany [a], Steven P. Oncley [a], Andrew A. Turnipseed [a], Britton B. Stephens [a], Donald H. Lenschow [a], Margaret A. LeMone [a], Russell K. Monson [b], Dean E. Anderson [c]

[a] *National Center for Atmospheric Research, Boulder, CO, USA*
[b] *University of Colorado, Boulder, CO, USA*
[c] *U.S. Geological Survey, Denver, CO, USA*

Received 1 November 2006; accepted 15 February 2007

Abstract

CO_2 transport processes relevant for estimating net ecosystem exchange (NEE) at the Niwot Ridge AmeriFlux site in the front range of the Rocky Mountains, Colorado, USA, were investigated during a pilot experiment. We found that cold, moist, and CO_2-rich air was transported downslope at night and upslope in the early morning at this forest site situated on a $\sim 5\%$ east-facing slope. We found that CO_2 advection dominated the total CO_2 transport in the NEE estimate at night although there are large uncertainties because of partial cancellation of horizontal and vertical advection. The horizontal CO_2 advection captured not only the CO_2 loss at night, but also the CO_2 uptake during daytime. We found that horizontal CO_2 advection was significant even during daytime especially when turbulent mixing was not significant, such as in early morning and evening transition periods and within the canopy. Similar processes can occur anywhere regardless of whether flow is generated by orography, synoptic pressure gradients, or surface heterogeneity as long as CO_2 concentration is not well mixed by turbulence. The long-term net effect of all the CO_2 budget terms on estimates of NEE needs to be investigated.

Keywords: Canopy; Carbon dioxide; Complex terrain; Drainage flow

1. Introduction

The role of greenhouse gases, especially CO_2, in global warming has drawn increasing attention in the climate community. Various observational studies on atmospheric CO_2 concentrations, oceanic CO_2 partial pressure, isotopic ratios of CO_2, and O_2 indicate that a large amount of CO_2 may be absorbed by the terrestrial ecosystems of the Northern Hemisphere (Tans et al., 1990; Ciais et al., 1995; Fan et al., 1998; Bousquet et al., 2000). Because the long-term CO_2 budget over terrestrial ecosystems relies on small differences between CO_2 uptake by ecosystems, and anthropogenic and natural CO_2 releases, accurate measurements of CO_2 transport are difficult. Since they are crucial for climate-change studies, currently there are over four hundred towers worldwide dedicated to monitoring the long-term CO_2 balance over various surface types. Net ecosystem exchange (NEE) is estimated by monitoring time variations of vertical turbulent transport and profiles of CO_2 at isolated towers. Yet CO_2 from both ecosystem respiration and air pollution can be transported horizontally as well as vertically, and is taken up by the ecosystem regardless of where the CO_2 is from. As NEE is estimated as the residual from the CO_2 budget equation, advection terms, which measure CO_2 changes along the wind direction, are missed in

* Corresponding author. Fax: +1 303 497 8994.
E-mail address: jsun@ucar.edu (J. Sun).

0168-1923/$ – see front matter
doi:10.1016/j.agrformet.2007.02.007

single tower measurements. Therefore, processes that lead to significant CO_2 advection and their impacts on estimates of NEE need to be investigated.

The importance of CO_2 advection in the CO_2 budget was apparently first conjectured based on observations of ''missing'' CO_2 at night (e.g., Wofsy et al., 1988; Goulden et al., 1996; Jarvis et al., 1997). It is well known that orographic flow at night is important (Mahrt and Larsen, 1990; Whiteman, 2000; Mahrt et al., 2001), even over a slope as small as 0.1° (Brost and Wyngaard, 1978). Dynamic aspects of nighttime drainage flow were investigated extensively in many field studies (e.g., Ellison and Turner, 1959; Horst and Doran, 1986; Rao et al., 1991; May and Wilczak, 1993; Van Gorsel et al., 2003). A series of atmospheric studies in complex terrain (ASCOT) field experiments in the 1980's investigated evening- and morning-transition wind, turbulence and temperature fields in valleys, valley tributaries on side-slopes, and interactions between valley and large-scale flows (Orgill and Schreck, 1985; Clements et al., 1989). Similarly, daytime orographic flow has been investigated through field campaigns and numerical modeling (e.g., Banta and Cotton, 1981; Toth and Johnson, 1985; Kondo et al., 1989; Helmis et al., 1990; King, 1997; Kossmann et al., 1998). All of the previous studies on orographic flow have been focused on its dynamic characteristics and its role in transporting polluted air, and on some aspects of water vapor transport over relatively open terrain slopes (Banta, 1982; Parrish et al., 1990).

Flow within canopies was traditionally studied over flat terrain (Kaimal and Finnigan, 1994; Finnigan, 2000), where the kinetic energy is transported to the canopy layer solely by synoptic flow; and over an idealized hill, where the kinetic energy was affected by hydrodynamic pressure gradients induced by the hill (Finnigan and Belcher, 2004; Finnigan, 2004a). In reality, the kinetic energy within canopies can be supplied by synoptic energy transport through the canopy top modulated by hydrodynamic (hill topography induced) and hydrostatic (hill thermodynamically induced) pressure gradients.

Schimel et al. (2002) suggested that 70% of the western U.S. carbon sink occurs at elevations above 750 m, where 50–85% of the land is dominated by hilly or mountainous topography. The role of orographic flow in transporting CO_2 at night has been investigated recently in the biogeoscience community (Yi et al., 2000; Lee and Hu, 2002; Staebler and Fitzjarrald, 2004; Lee, 2004; Finnigan, 2004a; Yi et al., 2005). Sun et al. (1998) investigated nocturnal CO_2 transport over a lake using aircraft measurements, and found significant advection from both lake and land breezes. Lee (1998) estimated vertical advection of CO_2 from a single tower. This was followed by numerous papers: Finnigan (1999), Baldocchi et al. (2000), and Kominami et al. (2003) among others also pointed out that neglecting horizontal advection of CO_2 in long-term CO_2 observation programs could unbalance the CO_2 budget. Aubinet et al. (2003), Staebler and Fitzjarrald (2004), Feigenwinter et al. (2004), Aubinet et al. (2005), Marcolla et al. (2005), and Wang et al. (2005) have all conducted field experiments that focused on the role of CO_2 advection on the CO_2 budget.

Aubinet et al. (2003) claimed that the nocturnal CO_2 concentration decreased downstream along the orographic flow at night due to entrainment of low CO_2 from above the canopy; however, their frequency distribution of the horizontal CO_2 gradient showed the opposite most of the time under stable conditions, which they considered as a systematic error. Staebler (2003) suggested that vertical advection was not as important as horizontal advection in the CO_2 budget. Staebler and Fitzjarrald (2004) found that a CO_2 deficit existed even when horizontal CO_2 advection is considered. Marcolla et al. (2005) found that the signs of the vertical and horizontal advection were related to friction velocity. Aubinet et al. (2005) compared CO_2 advection measured at six sites and found that the sign of horizontal CO_2 advection varied at different sites. Meanwhile, numerical simulations over complex terrain by Katul et al. (2006) showed delicate balance between horizontal and vertical CO_2 advection in determining CO_2 sources and sinks.

Difficulties in studying the CO_2 budget over complex terrain are the CO_2 advection and horizontal turbulent flux divergence. Both advective flux and turbulent flux divergence terms involve obtaining accurate temporal and spatial variations of wind and CO_2 concentration, especially over heterogeneous landscapes and complex terrain. In this study, we investigate fundamental methodology of how to calculate NEE using the CO_2 budget method with observations over heterogeneous and complex terrain. We focus on diurnal CO_2 transport mechanisms over the complex terrain that affect estimating NEE day and night. Characteristics of spatial and temporal variations of orographic flow and CO_2 concentrations at the long-term Niwot Ridge AmeriFlux tower site are discussed in Section 3. Diurnal CO_2 transport and its impacts on measurements of NEE are studied in Section 4. Discussions and summary are given in Section 5.

2. Observations

The Niwot Ridge experiment (NIWOT02) was conducted in Roosevelt National Forest in the Rocky Mountains of Colorado (40°1′58.4″N, 105°32′47″W, and 3050 m above sea level) during all of September 2002 (Fig. 1 a). The site is on the east slope of the Rocky Mountains with a mean slope ∼5% to the east. The site is dominated by Engelmann spruce (*Picea engelmannii*), subalpine fir (*Abies lasiocarpa*), limber pine (*Pinus flexilis*), and lodgepole pine (*Pinus contorta*) (Veblen, 1986; Anderson and Turnipseed, 2001; Monson et al.,

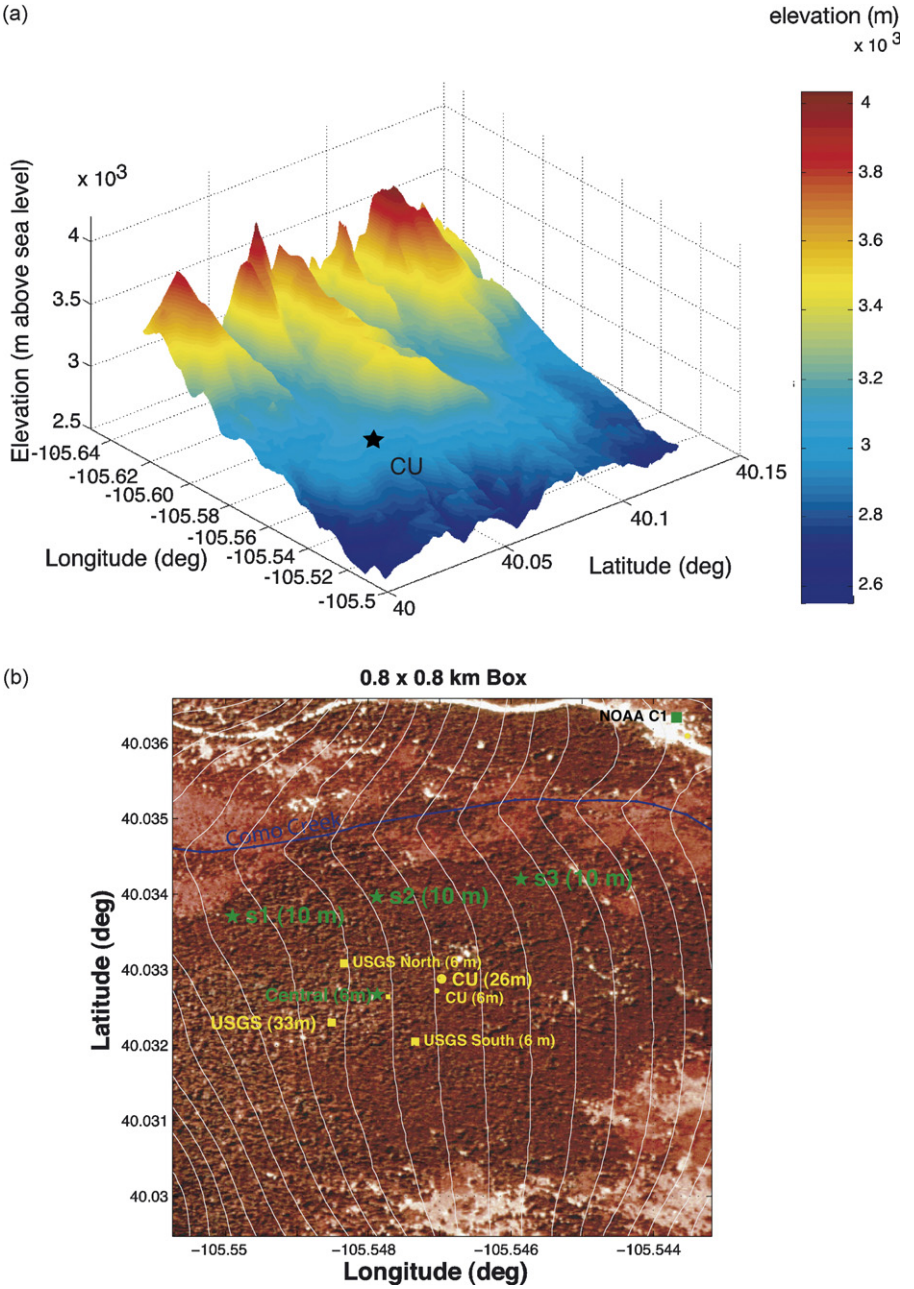

Fig. 1. (a) The Niwot Ridge AmeriFlux site at the east slope of the Rocky Mountains in Colorado. (b) A plan view of all the towers during the Niwot Ridge pilot experiment. The dark area on the remotely-sensed Infrared Orthophoto map corresponds to densely forested areas, while light areas are open, low-canopy, and shrub surfaces. The yellow labels are the existing towers during the NIWOT02 and the green labels are the supplemental towers.

2002; Turnipseed et al., 2002, 2003; Scott-Denton et al., 2003; Turnipseed et al., 2004; Yi et al., 2005). The typical tree height is 11.4 m with a leaf area index of 4.2 m^2m^{-2}. Climatology of the Niwot Ridge site has been studied by Barry (1973) and Brazel and Brazel (1983).

The AmeriFlux research site at Niwot Ridge contains six instrumented towers (Fig. 1b). The University of Colorado (CU) has operated two towers since 1998: a 26-m scaffolding tower and a 6-m triangular shaped tower, separated by about 20 m (Fig. 2 a). The U.S. Geological Survey (USGS) operates four towers: a 33-

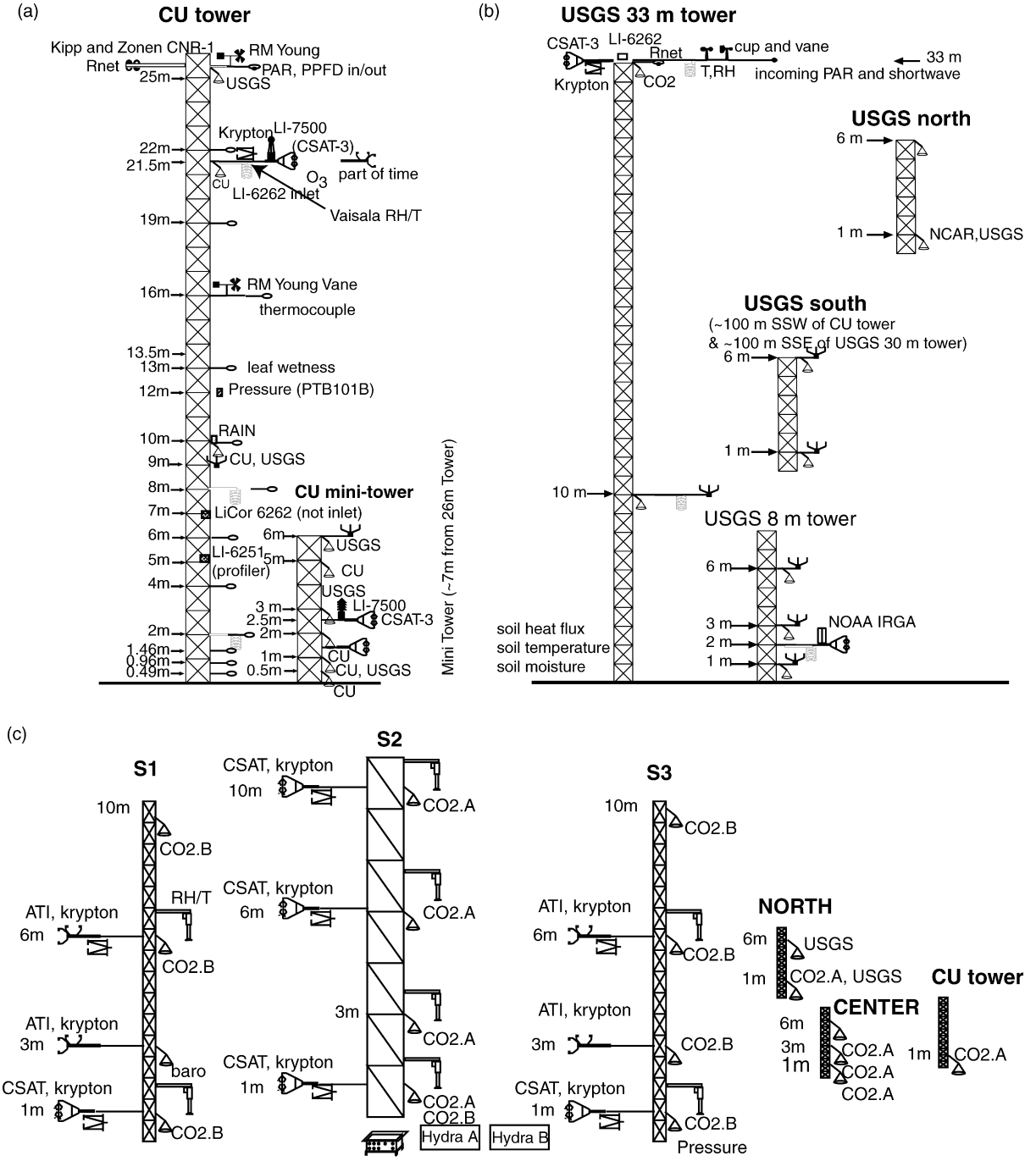

Fig. 2. Schematics of the towers operated by (a) CU, (b) USGS, and (c) NCAR during the NIWOT02.

Table 1
Sensors on the CU and USGS towers in September 2002

Towers	Sensors	Height (m)	Manufacturer	Model
CU	CO_2	0.5, 1, 2, 6, 10, 21.5	LI-COR	LI-6251
	T/RH	2, 8, 21.5	Vaisala	HMP35D
	U, V	6, 9	Vaisala	2-D Handar
	U, V	16, 25.5	RM Young	09101 prop vane
	u, *v*, *w*	1.5,2.56, 21.5	Campbell	CSAT-3
	Pressure	12	Vaisala	PTB220B
	Up & down long-, short-wave rad.	25.5	Kipp & Zonen	CNR-1
	Net radiation	25.5	REBS	Q*7.1
	PAR	25.5	LI-COR	LI-190SA
	Precipitation	10	Met One	#385-L
	Leaf wetness	13.5	Campbell	237-L
	Fast CO_2/H_2O	2.56, 21.5	LI-COR	LI-7500
	Fast H_2O	21.5	CSI Krypton	KH2O
	Fast CO_2	21.5	LI-COR	LI-6262
	Thermocouple	0.49, 0.96, 1.46, 2, 4, 6, 8, 10,13,16,19,22	Omega	E-type Thermocouples
USGS	Fast CO_2	33	LI-COR	LI-6262
	Fast CO_2	2	NOAA	IRGA
	CO_2	1, 3, 6, 10, 33	LI-COR	LI-7000
	U, V	1, 2, 3, 6, 10	Vaisala	2-D Handar
	u, *v*, *w*	33	Campbell	CSAT-3
	T/RH	2, 10, 33	Vaisala	HMP35-D
	Net radiation	33	REBS	Q*6
	Incoming shortwave	33	LI-COR	LI200
	Pressure	1	Vaisala	PTB101B
South	CO_2	1, 6	LI-COR	LI-7000
	U, V	1, 6	Campbell	2-D Handar
North	CO_2	1, 6	Campbell	LI-7000

T/RH = temperature and relative humidity; U,V = slow response eastward and northward wind components; *u*, *v*, *w* = fast response three-dimensional wind components; PAR = photosynthetic active radiation.

m tower, an 8-m tower, and two 6-m towers, i.e. north and south towers (Fig. 2b). The 33-m and 8-m towers are about 4 m apart. During the NIWOT02, four additional 10-m towers (s1, s2, s3, and central) were deployed by the National Center for Atmospheric Research (NCAR) to supplement the existing measurements (Fig. 2c). Tower s2 was a scaffolding tower, and the rest of the towers were triangular. All sensors on the CU and USGS towers during the NIWOT02 are listed in Table 1, and all the supplementary sensors are listed in Table 2.

CO_2 concentration was measured by a single infrared gas analyzer at both CU (LI-6251) and USGS (LI-7000) towers. Two calibration gases were used to ensure the absolute accuracy of CO_2 measurements every 2 h at USGS towers, and 4 h at the CU tower. In addition, water vapor was removed before air was sampled at the CU tower. Supplemental CO_2 concentration measurements were obtained from a set of 18 inlets ducted to a centralized CO_2 analyzing system consisting of two Li-7000 CO_2/H_2O analyzers we refer to as the ''HYDRA'' system (Burns et al., 2006). The 18 inlets were distributed throughout an area of about 0.3 km × 0.3 km. Xu et al. (1999) and Staebler (2003) deployed similar systems, but here three calibration gases (283.4, 360.1 and 419.5 ppm) were

Table 2
Sensors on supplemental towers at the Niwot Ridge site

Towers	Sensors	Height (m)	Manufacturer	Model
s1	CO_2	1, 3, 6, 10	LI-COR	LI-7000
	u, *v*, *w*	1	Campbell	CSAT-3
	u, *v*, *w*	3, 6	ATI	ATI-K
	Fast H_2O	1, 6	Campbell	KH20
	T/RH	1, 6	Vaisala/NCAR	50-Y
s2	CO_2	1, 3, 6, 10	LI-COR	LI-7000
	u, *v*, *w*	1, 6, 10	Campbell	CSAT-3
	Fast H_2O	1, 6, 10	Campbell	KH20
	T/RH	1,3, 6, 10	Vaisala/NCAR	50-Y
s3	CO_2	1, 3, 6, 10	LI-COR	LI-7000
	u, *v*, *w*	1	Campbell	CSAT-3
	u, *v*, *w*	3, 6	ATI	ATI-K
	T/RH	1, 6	Vaisala/NCAR	50-Y
	Fast H_2O	1, 6	Campbell	KH20
	Pressure	1	Vaisala	PTB220B
Central	CO_2	1, 3, 6	LI-COR	LI-7000

used to ensure accuracy of CO_2 measurements. In addition, water vapor was removed before air samples were analyzed. Due to the non-linear dependence of CO_2 concentration on temperature and pressure, using more calibration gases and conducting frequent calibrations significantly improves the relative and absolute measurement accuracy (Burns et al., 2006). Since the value of the first calibration gas, i.e. 283.4 ppm, was significantly lower than the lowest observed CO_2 concentration, we only use the other two calibration gases to calibrate CO_2 concentration measurements in this study. There were no fast-response CO_2 measurements on the supplemental towers. There were two fast-response CO_2 measurements (LI-6262 and LI-7500) at 21.5 m and one (LI-7500) at 2.56 m on the CU tower during the NIWOT02. The closed-path CO_2 analyzer (LI-6262) was calibrated every 4 h. Comparison between CO_2 fluxes from the open and closed-path analyzers at 21.5 m indicates that CO_2 fluxes were a little larger from the open-path analyzer (LI-7500) than from the close-path one. We have used fast-response CO_2 measurements from the open-path analyzer for this study.

To ensure consistency between the different CO_2 analyzing systems at the site, a mobile calibration system, consisting of four calibration gases (353.41, 369.47, 392.1, and 416.6 ppm) with calibrations traceable to the World Meteorological Organization (WMO) CO_2 scale, was periodically used to monitor the NCAR, CU, and USGS CO_2 analyzers. CO_2 concentration measurements at the NCAR, CU, and USGS sites were also continuously compared by co-locating a HYDRA inlet with a USGS inlet at the north tower at 1 m, and another inlet with one of the CU inlets at the CU tower at 1 m. The relative accuracy of CO_2 measured by the HYDRA (about ± 0.3 ppm) was determined from the mean CO_2 difference between two co-located inlets at 1-m height at s2, which were connected to two separate Li-7000 analyzers in the HYDRA system. Its absolute accuracy of about 1.5 ppm was determined by the mean difference between the HYDRA and the mobile calibration system. Using the co-located inlets at the CU and USGS north towers, the mean CO_2 measurement biases from the different analyzing systems during the NIWOT02 were removed by comparing their averaged CO_2 concentrations.

All the sonic anemometers were aligned with local gravity to within about 0.2° with bubble levels. In this study, the canopy layer is defined as the layer below the average tree top height. Averaging variables at a specific time of day over the entire NIWOT02 is called *composition* in this study to distinguish it from other types of averaging. Local Mountain Standard Time (MST), which is 7 h behind Coordinated Universal Time (UTC), is used in this study. Turbulent fluxes are calculated using the multiresolution decomposition method based on the diadic Harrwavelet transform as described by Howell and Mahrt (1997). The average time for defining turbulence perturbations is case-dependent to include all sizes of turbulent eddies and avoid non-turbulence influences (Vickers and Mahrt, 2003, 2006). CO_2 concentration was converted to mixing ratio (ppmv) in this study to avoid the influence of temperature fluctuations on turbulent CO_2 fluxes; therefore, the Webb correction is not needed here (Sun et al., 1995; Leuning, 2004). Turbulent fluxes are estimated as turbulent eddy covariances, i.e. kinematic fluxes, using the eddy correlation method.

3. Diurnal and spatial variations of orographic flow and CO_2 concentrations

3.1. Orographic flow

The detailed physical mechanism for development of downslope flow at night and upslope flow during daytime is described in the literature (e.g., Banta, 1982; Kondo and Sato, 1988; Kuwagata and Kondo, 1989; McKee and O'Neal, 1989; Geiger et al., 1995; Whiteman, 2000; Finnigan, 2004a). The composite hourly wind from the NIWOT02 shows that the diurnal variation of the orographic flow most likely occurred within the canopy layer, while synoptic westerlies were dominant above the canopy (Fig. 3). This result demonstrates that the flow within the canopy was strongly influenced by the hydrostatic pressure gradient associated with the radiative forcing of the topography instead of the downward momentum transport from the synoptic flow above the canopy as occurs over flat terrain.

The downslope westerly flow within the canopy was perpendicular to altitude contour lines from around 275°, i.e. the terrain slope direction, which was different from downslope synoptic westerlies above the canopy (Sun, 2007). The influence of the synoptic westerly flow and the orographic flow within the canopy highly depends on canopy density. Because s1 was at the boundary between the relatively open willow and the relatively closed evergreen forest areas, the thermal and roughness contrasts between the open and closed canopy areas led to relatively strong WNW flow at 1 m, the penetration of the synoptic westerly flow down to around 6 m within the canopy at night, and no obvious upslope flow even at 1 m during daytime

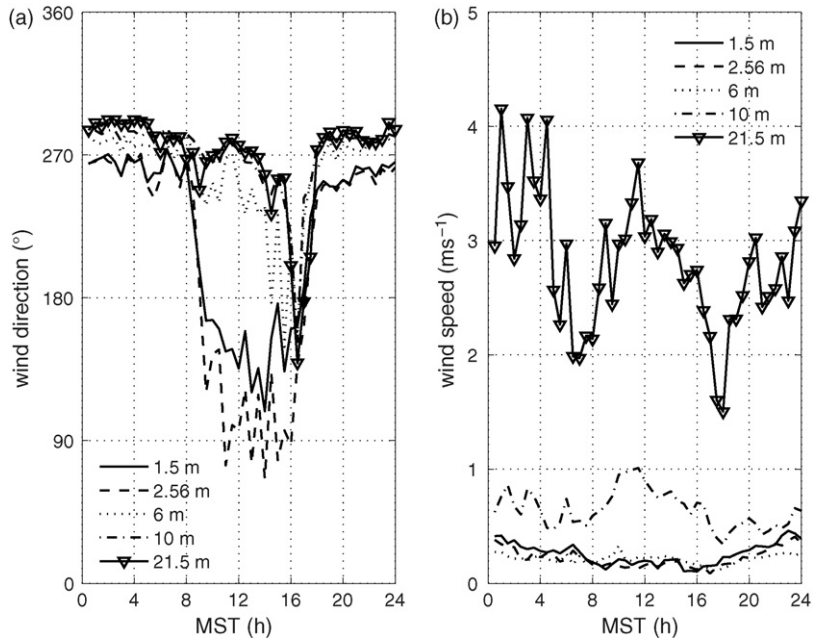

Fig. 3. The composite diurnal variation of (a) wind direction and (b) wind speed at the CU tower. The composite wind direction at each level was calculated using the averaged 30-min eastward and northward wind components in SRLEC (see Section 4 for the definition of the coordinates.)

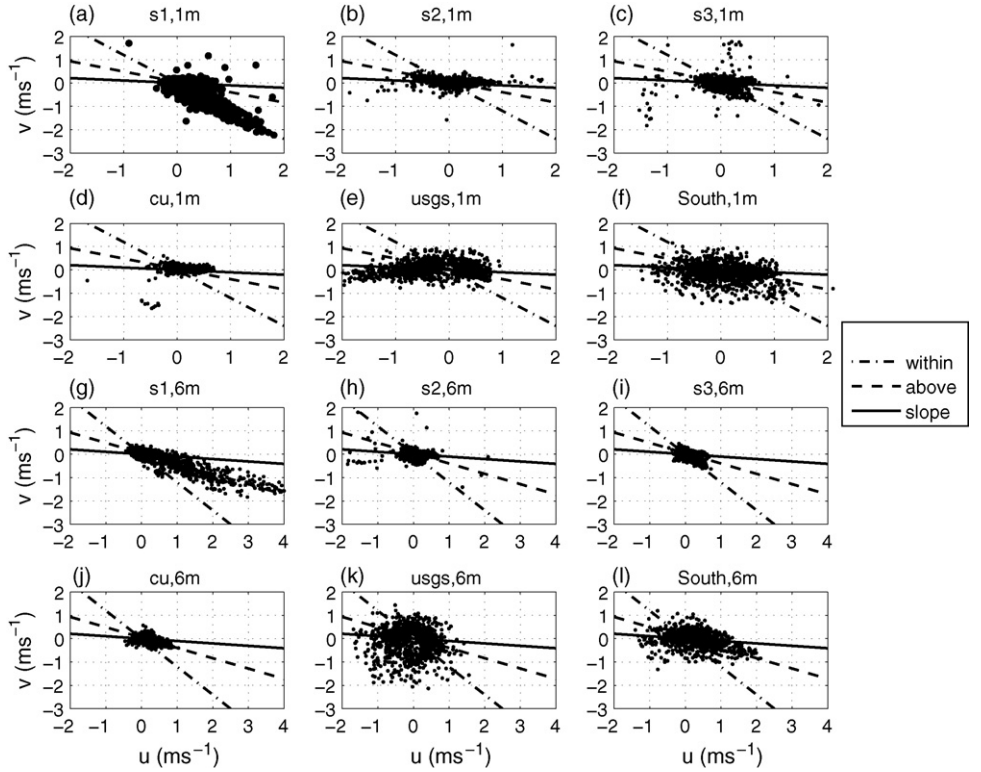

Fig. 4. The 30-min averaged eastward ($\bar{u}$) and northward ($\bar{v}$) wind components at 1 m at: (a) s1, (b) s2, (c) s3, (d) CU, (e) USGS, and (f) south tower; and at 6 m at: (g) s1, (h) s2, (i) s3, (j) CU, (k) USGS, and (l) south tower during the NIWOT02. The dominant wind directions within and above the canopy, and in the direction of the terrain slope are marked with dotted-dashed, dashed, and solid lines, respectively. Here wind components are in SRLEC.

(Fig. 4). At dense canopy spots, such as s2 and s3, the orographic flow was more effectively protected by the canopy and it was deeper (observable at 6 m) than relatively open canopy spots such as at CU and USGS. The wind direction at s2 and s3 sometimes deviated from the area terrain slope direction and turned northward towards nearby Como Creek. Due to the decoupling between the air within and above the canopy, the drainage flow toward Como Creek was evident within the canopy, but not above. Complications of decoupling between the canopy flow and the air above at a different site were discussed by Froelich et al. (2005) and Froelich and Schmid (2006).

Defining drainage flow as an organized flow at 1 m stronger than 0.4 m $s^{-1}$and from 275 ± 10°, we found at s2 that drainage flow events occurred throughout the night (Fig. 5). In contrast, most strong upslope events at s2, defined as the 1-m wind speed greater than 0.2 $ms^{-1}$and its direction from 90 ± 30°, occurred around noon when solar heating was strongest. The frequent occurrence of upslope flow around noon is consistent with the derivation by Hunt et al. (2003). Due to the prevailing synoptic westerly flow, the upslope easterly during daytime was weaker than the downslope westerly flow on the east slope of the Rocky Mountains (King, 1997), which was found during the NIWOT02 (Fig. 3). Nonetheless upslope flows were frequently observed in summer when the orographically induced thermal gradient was strongest (Toth and Johnson, 1985). A small percentage of upslope flows at night in Fig. 5 reflects the onset of drainage flow as described by Banta (1984), meandering weak wind within the canopy layer, and perhaps influences of synoptic hydrodynamic pressure gradients.

Although drainage flow prevails within the canopy layer, development of drainage flow is found to be closely related to weak synoptic westerlies under stably stratified conditions above the canopy. Using the bulk Richardson number ($R_i = g\Delta z\,\Delta\theta/(\bar{T}(\Delta U)^2)$, where g, Δz, $\Delta\theta$, ΔU, and $\bar{T}$, are the gravity constant, the layer depth, the potential temperature and wind speed differences across the layer, and the mean layer temperature) to characterize the hydrodynamical stability within and above the canopy layer, we found that strong drainage flow occurred when R_i was relatively large above the canopy layer and relatively small within it (Fig. 6 a). This difference in R_i implies decoupling between the air within and above the canopy.

At the Niwot Ridge site, the canopy is reasonably closed so that within the canopy layer, the air is better mixed at night than during daytime partly due to drainage flow, although the evening mixing is weak. As a result, the wind speed is weaker during the daytime

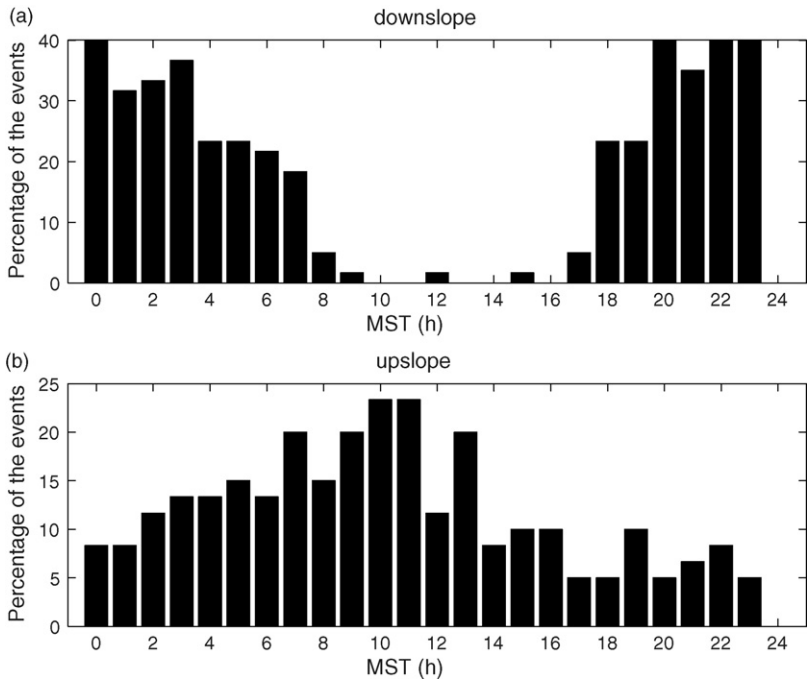

Fig. 5. Percentage of all the (a) downslope and (b) upslope events (30-min averaged flow) at each hour during the NIWOT02 that met the criteria defined in the text.

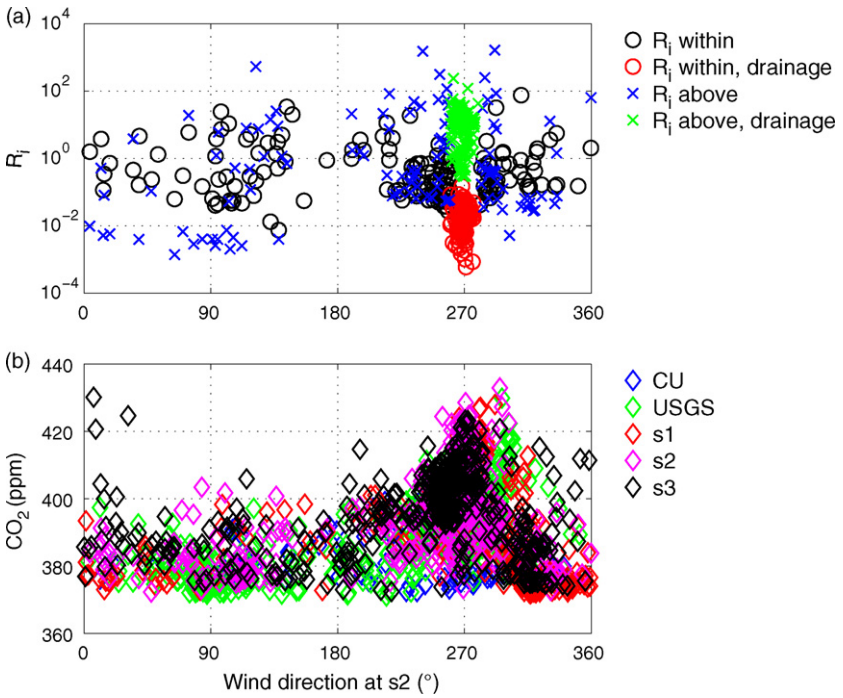

Fig. 6. (a) The bulk Richardson number (R_i) within and above the canopy layer with and without presence of drainage flow and (b) the CO_2 concentration at the five towers as a function of the wind direction at 1 m, s2 from 20 to 6 MST during the NIWOT02. Each symbol represents a 30-min averaged data point.

than at night (Fig. 3b). The wind speed profile within the canopy exhibited an ''S'' shaped pattern. The wind minimum is associated with large dissipation of the kinetic energy by the tree needles (Shaw, 1977), and its height is close to the 7.8-m displacement height at the CU tower found by Turnipseed et al. (2002) and the 8-m maximum leaf-density level found by Yi et al. (2005) during most of the day. Occasionally when the unstable layer reached the ground for several hours around noon, the height of the minimum wind speed decreased at the CU tower. The variation of S-shaped wind profiles at different towers is associated with spatial variations of the canopy density and the vertical distribution of the leaf area density.

3.2. CO_2 concentration

Plant roots and soil microbes are dominant producers of CO_2 efflux at the forest floor. Their CO_2 production depends on a number of environmental factors, such as soil organic content, moisture, temperature, oxygen and CO_2 concentrations, and nutrient availability, as well as a number of intrinsic factors, such as root biomass, and the size and composition of microbial populations (Glinski and Stepniewski, 1985; Moren and Lindroth, 2000; Monson et al., 2006). Overall, soil gases are transported mainly through two mechanisms: diffusion and mass flow (Kimball and Lemon, 1971). The diffusive flux is driven by the concentration gradient between the soil and the atmosphere, while mass flow is caused by a soil-atmosphere pressure gradient due to pressure pumping arising from air motion fluctuations and atmospheric pressure variations among other causes. In general, fluctuations in wind speed at the forest floor are relatively low compared to open areas; therefore, the mass flow is a weak contributor to CO_2 efflux. However, drainage or upslope flows can enhance the flow within the canopy and may increase the importance of the mass flow in the forest. Witkamp (1969) found that soil respiration normally varied with soil litter temperature, with a predawn minimum and an afternoon maximum. He also found that a second maximum occurred occasionally between midnight and dawn when cold air overlaid the relatively warm soil, leading to thermal mixing across the earth surface and release of CO_2-rich air from the soil to the atmosphere. This result implies that the soil respiration, either by diffusive or mass flow processes, can be enhanced by hydrostatic instability and pressure perturbations across the soil surface.

We found that the 1-m CO_2 concentration at all stations was highest when the wind was in the direction of drainage flow at night (Fig. 6b), implying that the

high CO_2 concentration could be the accumulation of soil respiration due to both mass flux and diffusive release of CO_2 enhanced by the cold drainage flow. As described in the previous section, the drainage flow occurs when the air above the canopy is very stable. The larger CO_2 concentration during the development of drainage flow also reflected the fact that more CO_2 was trapped close to the ground under more stable conditions. To minimize the random error associated with the CO_2 temporal fluctuations, we composited the diurnal variation of the CO_2 concentration at each tower during the NIWOT02. The spatial distribution of the composite CO_2 shows that nighttime CO_2 concentration increased toward Como Creek at 1 and 3 m, and increased down the terrain slope at 6 m (Fig. 7). Since CO_2 is transported by drainage flow at night, this result indicates that the drainage flow associated with Como Creek was confined to the lower part of the canopy layer, while the regional drainage flow is down the main terrain slope. Nakane (1975) investigated soil respiration under an evergreen oak forest from the valley bottom to the ridge of a hill and found that the soil respiration from the surface litter and mineral layers decreased with elevation. The higher CO_2 concentration towards low elevation at night implies that locally respired high CO_2 is constantly replaced by remotely

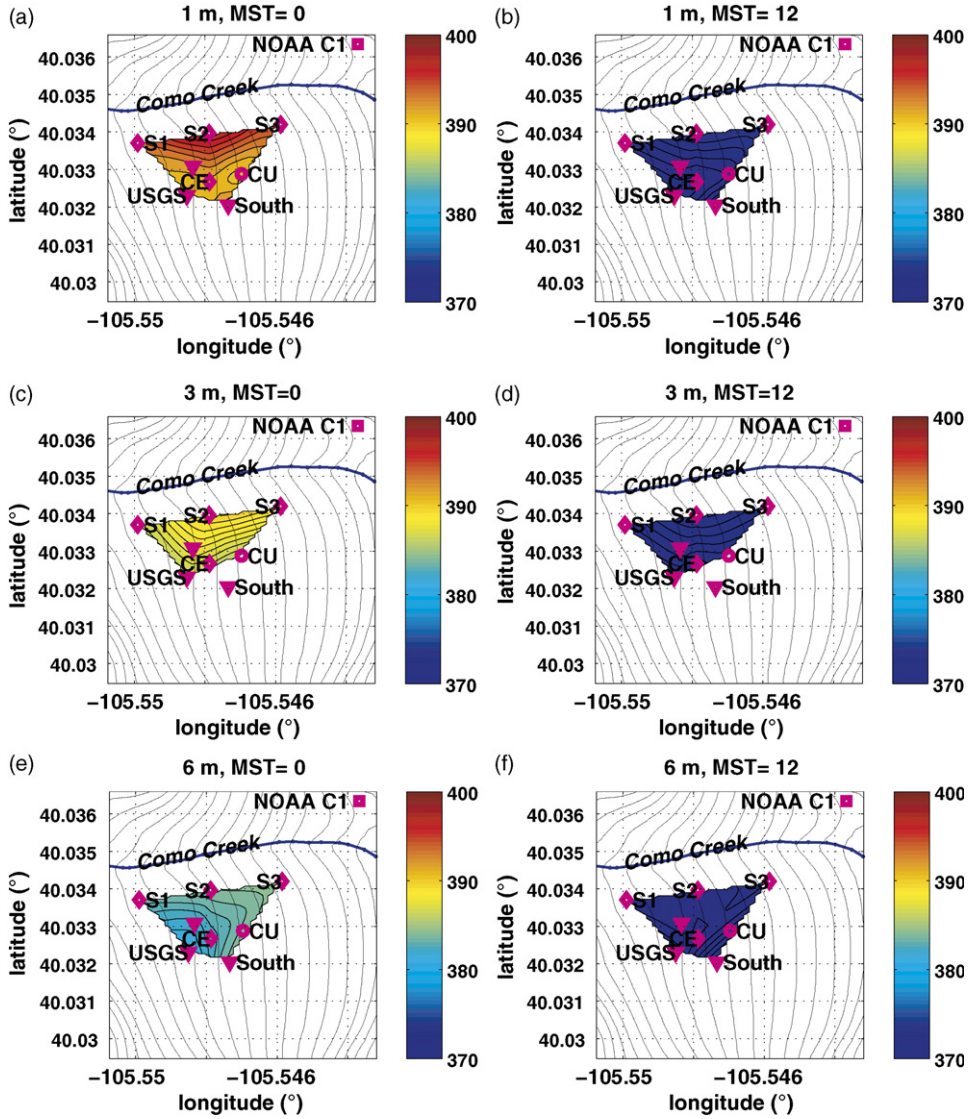

Fig. 7. The spatial distributions of the composite CO_2 concentration during the NIWOT02 at 1 m (a and b), 3 m (c and d), and 6 m (e and f) at 0 and 12 MST.

respired low CO_2 from high ground by drainage flow at night. This drainage flow transport over long distances could partly explain the "missing" CO_2 myth as most of the real world is not flat. The CO_2 concentration and its spatial variation were much less during daytime than nighttime, however, a small consistent reduction of the CO_2 concentration in the upslope direction is detectable (more in next section).

As discussed above, orographic flow depends on decoupling between the air above and below the canopy at the site. Turbulent mixing from gust fronts can reduce the decoupling and has significant impacts on spatial distributions of CO_2, which was evident on 24 September 2002 (Fig. 8). As a wind gust arrived in the middle of the night, the creek-ward drainage flow was eliminated by turbulent mixing generated by the wind gust but the terrain slope drainage flow remained. Consequently, the high CO_2 along Como Creek before the arrival of the wind gust disappeared and relatively high CO_2 was found down the main terrain slope after the onset of the wind gust.

4. CO_2 budget

The volume-averaged CO_2 budget can be expressed via the mass balance equation in Cartesian

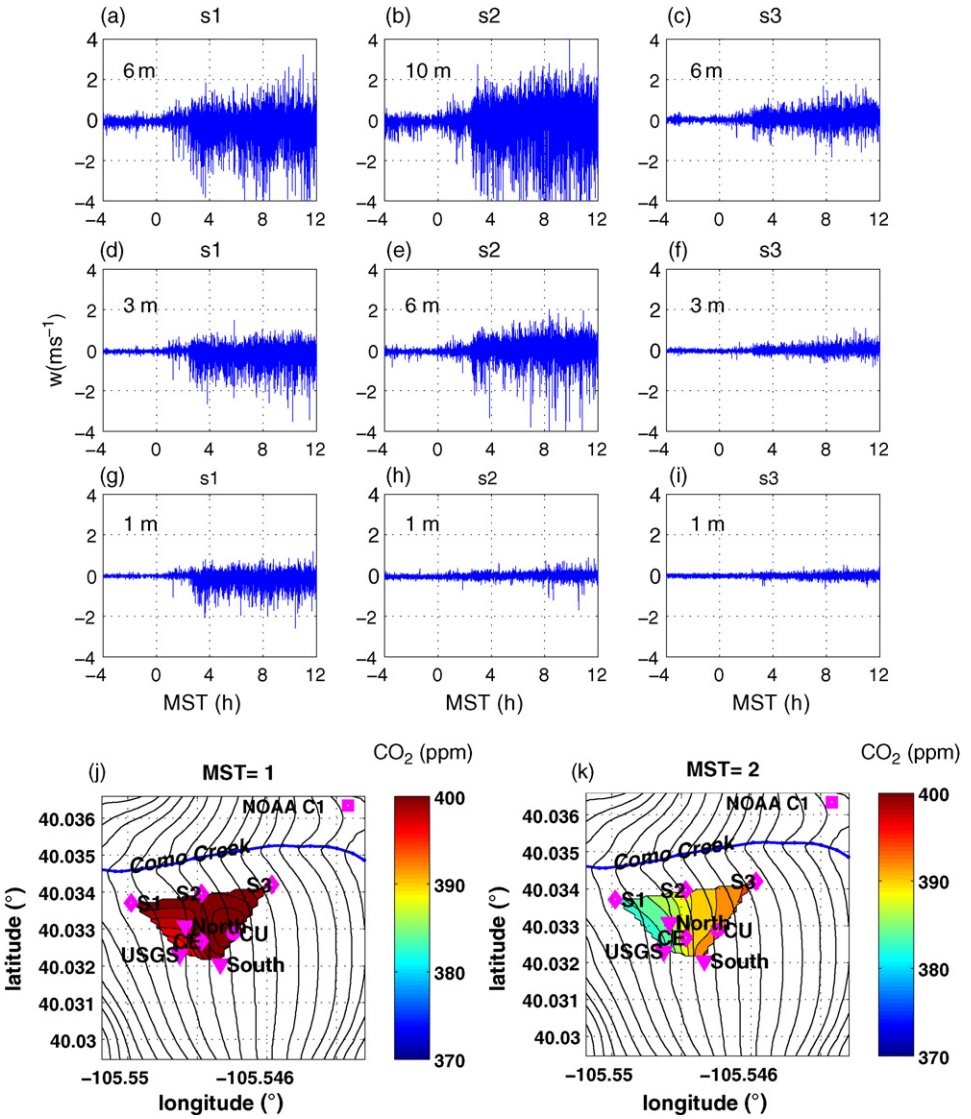

Fig. 8. Time series of the vertical velocity at s1 (a, d and g), s2 (b, e and h), and s3 (c, f and i) at various heights and spatial variation of CO_2 concentration before (j) and after (k) a wind gust on 24 September. The plot demonstrates the timing and penetration of the wind gust and its influence on the spatial variation of CO_2 concentration.

coordinates as:

$$\int_0^z \int_{y_1}^{y_2} \int_{x_1}^{x_2} \left[\frac{\partial \bar{c}}{\partial t} + \bar{u}\frac{\partial \bar{c}}{\partial x} + \bar{v}\frac{\partial \bar{c}}{\partial y} + \bar{w}\frac{\partial \bar{c}}{\partial z} + \frac{\partial \overline{u'c'}}{\partial x} + \frac{\partial \overline{v'c'}}{\partial y} + \frac{\partial \overline{w'c'}}{\partial z} \right] \mathrm{d}x\,\mathrm{d}y\,\mathrm{d}z \equiv \int_{y_1}^{y_2} \int_{x_1}^{x_2} [C_{\text{storage}} + C_{x\text{adv}} + C_{y\text{adv}} + C_{z\text{adv}} + C_{x\text{f}} + C_{y\text{f}} + C_{z\text{f}}]\,\mathrm{d}x\,\mathrm{d}y = S, \quad (1)$$

where c is the CO_2 concentration, S is the CO_2 source/sink, and the vertical integration is from the ground to an observation height. The overline and prime terms represent time averaged and temporal perturbation quantities. The terms on the left hand side of Eq. (1) represent storage (tendency in meteorology), advection in x, y and z directions, and turbulent flux divergence in x, y, and z directions, respectively; and the terms with subscripts are their corresponding vertically integrated terms.

Based on (1), NEE from a box region can be expressed as

$$\mathrm{NEE} \equiv \int_{y_1}^{y_2} \int_{x_1}^{x_2} \left(\overline{w'c'}_0 + \int_0^z S\,\mathrm{d}z \right) \mathrm{d}x\,\mathrm{d}y = \int_{y_1}^{y_2} \int_{x_1}^{x_2} \left[\int_0^z \left(\frac{\partial \bar{c}}{\partial t} + \bar{u}\frac{\partial \bar{c}}{\partial x} + \bar{v}\frac{\partial \bar{c}}{\partial y} + \bar{w}\frac{\partial \bar{c}}{\partial z} + \frac{\partial \overline{u'c'}}{\partial x} + \frac{\partial \overline{v'c'}}{\partial y} \right) \mathrm{d}z + \overline{w'c'}_z \right] \mathrm{d}x\,\mathrm{d}y \equiv \mathrm{NEE}_i + \mathrm{NEE}_m, \quad (2)$$

where

$$\mathrm{NEE}_i \equiv \int_{y_1}^{y_2} \int_{x_1}^{x_2} \left(\int_0^z \frac{\partial \bar{c}}{\partial t} + \overline{w'c'}_z \right) \mathrm{d}x\,\mathrm{d}y, \quad (3)$$

$$\mathrm{NEE}_m \equiv \int_{y_1}^{y_2} \int_{x_1}^{x_2} \left[\int_0^z \left(\bar{u}\frac{\partial \bar{c}}{\partial x} + \bar{v}\frac{\partial \bar{c}}{\partial y} + \bar{w}\frac{\partial \bar{c}}{\partial z} + \frac{\partial \overline{u'c'}}{\partial x} + \frac{\partial \overline{v'c'}}{\partial y} \right) \mathrm{d}z \right] \mathrm{d}x\,\mathrm{d}y = \int_{y_1}^{y_2} \int_{x_1}^{x_2} \left[C_{x\text{adv}} + C_{y\text{adv}} + C_{z\text{adv}} + C_{x\text{f}} + C_{y\text{f}} \right] \mathrm{d}x\,\mathrm{d}y. \quad (4)$$

The term $\overline{w'c'}_0$ in (2) represents soil respiration, NEE_i and NEE_m represent the NEE estimated using CO_2 profiles and eddy correlation measurements from an isolated tower, and the additional terms associated with CO_2 advection, respectively.

By applying the continuity equation,

$$\frac{\partial \bar{u}}{\partial x} + \frac{\partial \bar{v}}{\partial y} + \frac{\partial \bar{w}}{\partial z} = 0, \quad (5)$$

the advection terms in (1) can be rewritten as

$$\bar{u}\frac{\partial \bar{c}}{\partial x} + \bar{v}\frac{\partial \bar{c}}{\partial y} + \bar{w}\frac{\partial \bar{c}}{\partial z} = \frac{\partial(\bar{u}\bar{c})}{\partial x} + \frac{\partial(\bar{v}\bar{c})}{\partial y} + \frac{\partial(\bar{w}\bar{c})}{\partial z}. \quad (6)$$

If the continuity equation is satisfied with observed wind components, there is no difference between the advection formula on the left and right sides of (6). Due to temporal and spatial variations of wind and CO_2 concentration, and instrument errors, relative uncertainties in calculating the horizontal CO_2 advection are

$$\frac{1}{\bar{u}\,\bar{c}}(\bar{u}\delta\bar{c}) = \frac{\delta\bar{c}}{\bar{c}}, \quad (7)$$

if it is expressed as on the left side of (6), and

$$\frac{1}{\bar{u}\,\bar{c}}\delta(\bar{u}\,\bar{c}) = \frac{\delta\bar{u}}{\bar{u}} + \frac{\delta\bar{c}}{\bar{c}}, \quad (8)$$

as on the right side of (6), where δ represents the uncertainty in horizontal differences. Since the relative variation of wind is much larger than that for CO_2 concentration, i.e. $\delta\bar{u}/\bar{u} \gg \delta\bar{c}/\bar{c}$, the CO_2 advection expressed on the left side of (6) would be less sensitive to temporal and spatial variations of wind than that expressed on the right side of (6). As a result of spatial and temporal variations of wind and numerical errors in calculating all the terms in the mass balance (5), using the two formulae may lead to different results. In this study, we use the advection formula at the left side of (6) to investigate the contribution of the advection to the CO_2 budget.

As discussed in Sun (2007), due to the dynamic nature of flow over complex terrain, it is difficult to specify a fixed control volume relative to the earth in flow-dependent streamline coordinates, with which multiple sonic anemometers are used for the CO_2 budget calculation. In this study, we use slope-referenced local earth coordinates (SRLEC) to approximate local earth coordinates. Local earth coordinates are Cartesian coordinates with eastward as x, northward as y, and upward normal to the geopotential surface as z directions (Fig. 9). We assume that all the sonic anemometers used in this study were approximately aligned with local gravity, and SRLEC are obtained by slightly adjusting the ratio of their vertical wind to horizontal wind in the direction normal to topographic contours according to the pre-determined terrain slope. We analyzed all the sonic anemometer data used in this study and determined the terrain slope and the direction of the terrain slope (normal to topographic contours) by using flow data when they were parallel to the local slope (relationship between vertical and horizontal wind does not vary with wind direction).

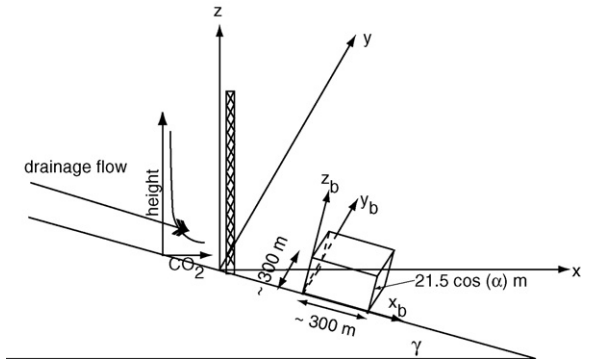

Fig. 9. The axes of SRLEC in eastward (x), northward (y), and vertical (z) directions and the box used to estimate the NEE using the CO_2 budget equation.

We chose a rectangular box for estimating NEE with its horizontal plane parallel to the terrain slope ($\gamma \sim 4.3°$), its horizontal axis, x_b, along the terrain slope direction ($\sim 275°$), and its vertical direction normal to the terrain slope (Fig. 9). The box is chosen to cover the measurement area of all the towers during the NIWOT02, which is about 300 m × 300 m in its horizontal plane and zero to 21.5 $\cos\gamma$ m above the ground in its vertical direction. Recognizing that wind was observed approximately in SRLEC, but CO_2 concentration was measured relative to the ground, i.e. along the terrain slope and along the towers in vertical, we decompose all the necessary wind components and CO_2 concentration into box coordinates for calculation of NEE. Therefore, horizontal (along the $x_b \times y_b$ plane in Fig. 9) and vertical (in the direction of z_b in Fig. 9) CO_2 transports are referenced to the box from now on.

In this study, we estimate all the terms that contribute to NEE with emphasis on NEE_m except the horizontal turbulent flux divergence terms within the box. We use water vapor as a surrogate for estimating the magnitude of vertically integrated horizontal turbulent flux divergence compared to the vertical turbulent flux. Since we observe CO_2 transport across the boundaries of the box and we are only interested in the CO_2 transport within the box, footprints of fluxes and concentrations (Schmid, 2002; Finnigan, 2004b) should not be issues here. During the one-month NIWOT02, the CU data system suffered a power outage and lost the fast-response CO_2 data, which we rely on for estimation of NEE. We focus only on 3 days, 14–16 September 2002, of typical weak to moderate winds for which we have all the necessary data.

4.1. CO_2 storage

To understand the vertical advection of CO_2 and the diurnal variation of CO_2 storage, we first investigated the diurnal variation of the CO_2 profile at the site. As the ground cools by longwave radiation emission at night, the air close to the ground becomes stably stratified, although the air was more stable above than within the canopy due to the radiative cooling at the top of canopy. The stable boundary layer prevents the ecosystem respired CO_2 from mixing upward, especially above the canopy. Consequently, the CO_2 concentration close to the ground steadily increases with time, resulting in an approximately exponential decrease of CO_2 with height. During the day, solar heating of the canopy leads to thermal instability and well-mixed CO_2 above the canopy layer. Daytime mixing penetrates through the canopy below the maximum leaf-density level depending on canopy density. Below that, the shaded ground maintains a stable layer and the CO_2 concentration decreases with height within the canopy throughout the day except several hours around noon at locations where canopies are not very dense such as the CU tower. As photosynthesis starts, CO_2 is removed and water vapor is released by leaves. Cooled leaves reduce thermal mixing, leading to CO_2 increases with height above the canopy. Some enhancement of turbulent mixing may occur due to wind-driven flapping motions of stems, branches, and leaves (Sun and Mahrt, 1995).

During daytime, the vertical distribution of CO_2 is similar at different tower locations. However, at night relatively large differences occur. We use CO_2 concentration profiles and eddy correlation measurements at the CU tower to estimate the vertical CO_2 advection and vertical turbulent flux within the box. Since all CO_2 concentration measurements were made by a single CO_2 analyzer (the CO_2 concentration at any inlet was sampled every 6 min at CU), the CO_2 storage was calculated using 30-min averaged concentration profiles although errors due to fast variations of CO_2 may be introduced as discussed by Finnigan (2006). In addition, since the CO_2 gradient is much larger in z than in x and y directions, especially at night, we only need to calculate the gradient in the z_b direction from the gradient in z direction for the storage calculation as well as for the vertical CO_2 advection calculation. We use the standard deviation of the CO_2 concentration observed at eight locations at 1 and 6 m at each half-hour to estimate error bars for the storage term.

4.2. Horizontal CO_2 advection

Since wind speed had a secondary maximum around 1 m above the ground and CO_2 increased rapidly towards the ground, the maximum horizontal advection of CO_2 within the canopy layer is at about 1 m. A similar result was found by Staebler and Fitzjarrald (2004). Because the horizontal CO_2 advection is sensitive to the spatial variation of CO_2 and wind, we interpolated CO_2 and wind observations from the eight towers (s1, s2, s3, north, south, central, CU, and USGS) to 50 × 50 grid points using a cubic fit at both 1 and 6 m. Assuming the averaged horizontal CO_2 advection between 1 and 6 m represents the mean horizontal CO_2 advection between the ground and the top of the box, the contribution of horizontal CO_2 advection can be vertically integrated from the ground to the top of the box. To test the sensitivity of the spatial variation of wind and CO_2 concentration to the box-averaged horizontal CO_2 advection, we use three different averaging methods for area-averaged horizontal CO_2 advection at both 1 and 6 m. For method 1, we sum products of wind and CO_2 horizontal gradient at every grid point, i.e. $\sum_i \sum_j (u_{ij}\partial c/\partial x|_{ij} + v_{ij}\partial c/\partial y|_{ij})$, where i and j are the grid indices in the x_b and y_b directions and all the variables are in box coordinates. For method 2, we integrate products of mean wind components and mean CO_2 gradients in both x_b and y_b directions, i.e. $\sum_j \bar{u}_j(\overline{\partial c/\partial x})_j + \sum_i \bar{v}_i(\overline{\partial c/\partial y})_i$. For method 3, we sum products of the area-averaged wind component and area-averaged CO_2 in x_b and y_b directions, i.e. $\bar{u}\overline{\partial c/\partial x} + \bar{v}\overline{\partial c/\partial y}$. We found that all three methods have similar diurnal variations for the three days: positive at night and negative during daytime, i.e. including the horizontal CO_2 advection increases the estimation of nighttime respiration and daytime CO_2 uptake (Fig. 10). Although spatial variations of CO_2 concentration are much less during daytime than at night, the consistent negative CO_2 advection for the three days indicates that CO_2 concentration decreased in the direction of the upslope flow due to canopy uptake throughout the daytime. Since the horizontal CO_2 decrease is associated with photosynthesis, it can exist even in homogeneous ecosystems over flat or sloping terrain. As long as canopies take up CO_2, CO_2 concentration has to decrease as flow passes through canopies regardless of whether or not the flow is associated with topography, unless the CO_2 decrease is quickly mixed upwards by turbulence. In that case, the CO_2 uptake is only reflected in vertical turbulent CO_2 flux.

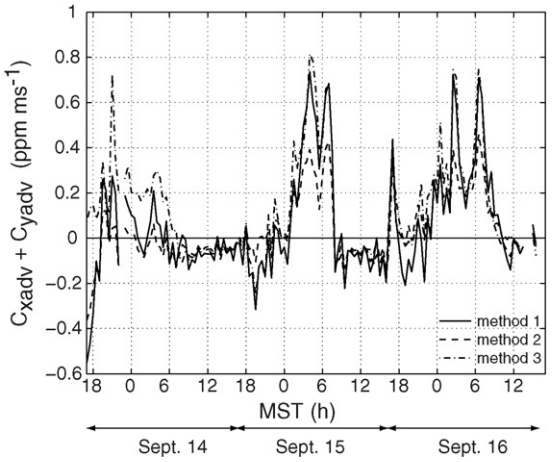

Fig. 10. Vertically integrated horizontal CO_2 advection ($C_{xadv} + C_{yadv}$) estimated for 14–16 September 2002. See text for the three methods.

4.3. Vertical CO_2 advection

As discussed in Sun (2007), the averaged streamline plane from the planar fit method is not parallel to the terrain slope at 21.5 m, which is similar to what was found by Froelich et al. (2005). The observed vertical velocity normal to the streamline plane derived from the planar fit method could have the opposite sign from the observed vertical velocity normal to the terrain slope, which in turns leads to the opposite vertical CO_2 advection. Although the observed vertical velocity normal to the slope decreases with decreasing height, the vertical CO_2 gradient increases with decreasing height, especially at night. Therefore, the vertical CO_2 advection is sensitive to the vertical variation of both vertical velocity and the CO_2 gradient especially within the canopy where the vertical gradient is strong at night. Our data indicate that the vertical velocity within the canopy can be noticeably smaller than above. To best use the three sonic anemometers at 1.5, 2.56, and 21.5 m at the CU tower, we assume that the vertical velocity decreases linearly from 1.5 m to zero at the ground, but remains constant from 2 to 10 m (∼ top of the canopy), and linearly increases from 10 to 21.5 m. The vertical CO_2 gradient is estimated using the CO_2 concentration observed at five levels (0.5, 1, 2, 5, 10, and 21.5 m) in the z direction rotated to z_b. The vertical CO_2 advection is then vertically integrated from the ground to the top of the box (Fig. 11). Due to the uncertainty of the regional terrain slope, we use the difference between the vertical velocity in SRLEC normal to the terrain slope and the vertical velocity from the planar fit method in estimating error bars for the vertical CO_2 advection.

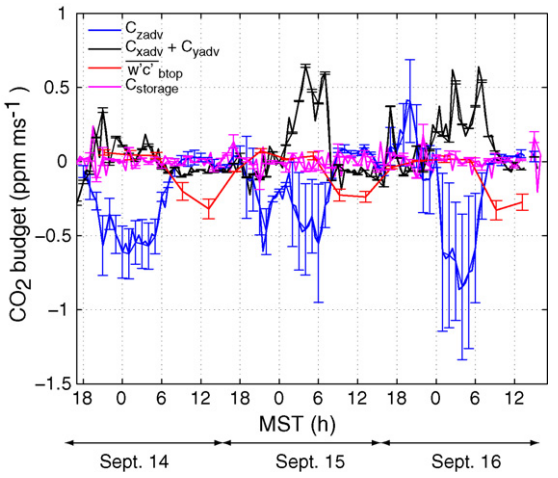

Fig. 11. The diurnal variation of the CO_2 storage ($C_{storage}$), vertically integrated horizontal ($C_{xadv} + C_{yadv}$) and vertical (C_{zadv}) CO_2 advection terms, and the vertical turbulent CO_2 flux normal to the top of the box ($\overline{w'c'}_{b\ top}$) for 14–16 September. The vertically integrated horizontal advection averaged among the three methods is plotted here.

4.4. Horizontal and vertical turbulent CO_2 transport

Although flow within and above the canopy is decoupled and the vertical turbulent CO_2 flux varies with height, we only need to estimate the vertical turbulent CO_2 flux at the observational level to investigate NEE as shown in Eq. (2). We do need to consider the vertical variation of the horizontal turbulent CO_2 flux divergence for C_{xf} and C_{yf}.

4.4.1. Vertical turbulent CO_2 transport

Vertical turbulent fluxes of CO_2 normal to the top of the box are calculated using the eddy correlation method with measurements at 21.5 m from the CU tower and are obtained by simply integrating cospectra of vertical velocity and CO_2 over eddy sizes (or frequency). Although the vertical velocity normal to the terrain slope is different from the vertical velocity normal to the streamline plane derived from the planar fit method at 21.5 m, the covariance between the vertical velocity and CO_2 concentration normal to the terrain slope and normal to the streamline plane is within 8% based on the 3-day dataset. The vertical CO_2 flux within the canopy layer was always upward both night and day (Fig. 12), which is consistent with the observed stable boundary layer and the net ecosystem CO_2 source there. The vertical CO_2 turbulent flux above the canopy was upward at night while stomata were closed, and downward during the day due to photosynthesis. Uncertainties in the vertical CO_2 turbulent

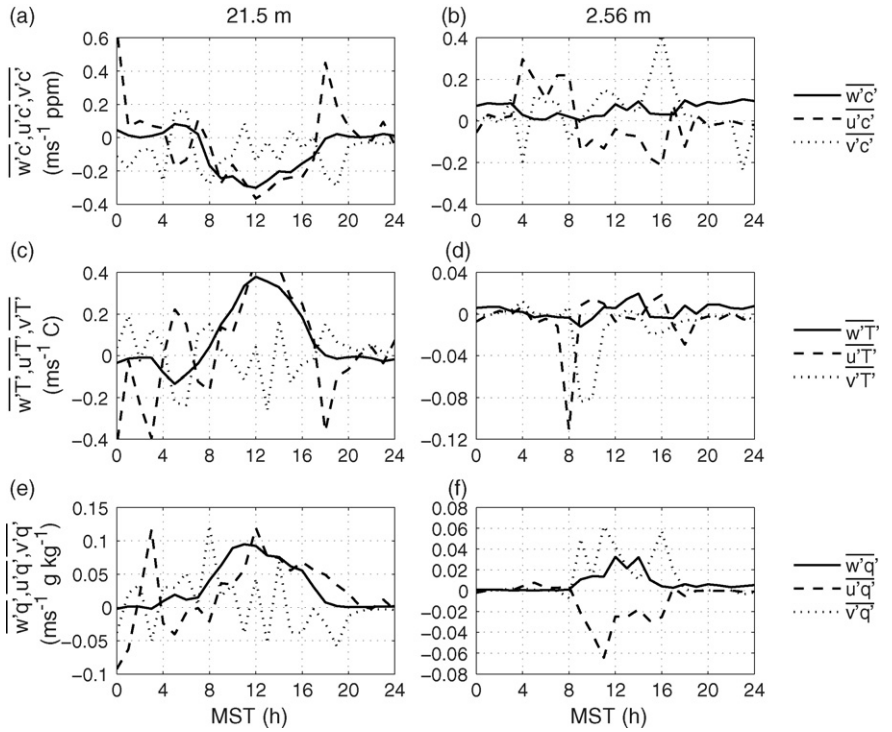

Fig. 12. The diurnal variation of the vertical and horizontal CO_2 turbulent fluxes (a and b), heat fluxes (c and d), and water vapor fluxes (e and f) at 21.5 m (left column) and 2.56 m (right column) at the CU tower for 15 September.

flux are estimated as the difference between the fluxes calculated using the two different CO_2 analyzers at 21.5 m.

4.4.2. Horizontal turbulent CO_2 transport

Overall, the magnitude of horizontal CO_2 turbulent flux ($\overline{u'c'}$) is comparable to the vertical flux, and its temporal variation is much larger than the vertical flux since horizontal fluxes are significantly affected by horizontal mesoscale meandering motions (Fig. 12). The horizontal CO_2 flux within and above the canopy was approximately downslope at night and upslope during the day, either along the terrain slope or along the local slope towards Como Creek, which is consistent with the diurnal variation of the slope flow at the site.

According to Staebler and Fitzjarrald (2004), the contribution of the horizontal turbulent transport of CO_2 to the total CO_2 budget could be the same order of the magnitude as the horizontal advection. In the absence of fast-response CO_2 measurements at different locations during the NIWOT02, we use water vapor as a surrogate to estimate the vertically integrated horizontal turbulent flux divergence ($C_{xf} + C_{yf}$) compared to the vertical CO_2 flux.

Before we examine the horizontal turbulent water vapor flux divergence, we investigate diurnal variations of horizontal turbulent water vapor flux and its relationship with horizontal CO_2 and temperature fluxes. We found that the direction of turbulent fluxes of water vapor and CO_2 were similar within the canopy layer day and night, but different above during the daytime (Fig. 12). Turbulent eddies transport cold, moist, CO_2-rich air downslope at night within and above the canopy layer. During daytime, turbulent eddies transport cold, CO_2-rich air upslope both within and above the canopy. However, upslope moisture flux is opposite within and above the canopy; i.e. turbulence transports moist air within but dry air above the canopy. Since horizontal turbulent flux of any trace gas can be generated through its vertical turbulent mixing and vertical wind shear (Wyngaard, 2004), or horizontal down-gradient transport, we investigated both possibilities for explanation of the observed horizontal CO_2 and water vapor fluxes. Since vertical wind shear right above the canopy is always positive due to the canopy drag on the flow, downward CO_2 and upward sensible and water vapor turbulent fluxes above the canopy during daytime would lead to positive horizontal CO_2 and negative heat and water vapor turbulent fluxes, which is opposite to what we observed. The result implies that the horizontal turbulent flux along the terrain slope is due to the horizontal down-gradient transport associated with the upslope flow. The upslope transport of dry air above the canopy during daytime could be associated with dry descending air as part of the local circulation associated with the upslope flow constrained by the continuity equation. As pointed out by Albertson and Parlange (1999), the relative importance of the horizontal to vertical turbulent transport of temperature can be significantly different from that for passive scalars, such as CO_2 and water vapor, and passive scalars tend to spread more horizontally compared to temperature. At our site, the magnitudes of the horizontal and vertical turbulent fluxes of either CO_2, or water vapor, or temperature are about the same.

Since towers s2 and s3 were located in similar canopy conditions, horizontal turbulent fluxes of water vapor at the two towers within the canopy (1 and 6 m) are used to estimate the horizontal turbulent water vapor flux divergence. The horizontal and vertical turbulent fluxes of water vapor have similar diurnal variations at the two sites although the horizontal water vapor flux has large fluctuations (Fig. 13). The vertically integrated horizontal turbulent water vapor flux divergence is comparable to the vertical turbulent flux of water vapor.

Although both CO_2 and water vapor are passive scalars, they have different sources/sinks. They are highly negatively correlated during photosynthesis when leaf stomata take up CO_2 and release water vapor. At night, CO_2 respiration can come from both soil and plants, while water vapor comes almost entirely from ground evaporation. Although both CO_2 respiration and evaporation depend on soil temperature and water content, CO_2 respiration also depends on internal and external soil factors as discussed in Section 3.2. Furthermore, CO_2 release is normally much smaller from water surfaces than from soil, while evaporation is opposite. Although CO_2 and water vapor have different sources/sinks, they should have similar transport properties once they are released into the air. Based on the characteristics of the turbulent water vapor transport, the magnitude of the vertically integrated horizontal turbulent CO_2 flux divergence could be comparable to the vertical turbulent flux and vary significantly with time as it is sensitive to variations of synoptic flow.

4.5. CO_2 transport in early morning and evening

The change in CO_2 concentration is greatest during the morning and evening transitions (Fig. 14 a). The large decrease in the CO_2 concentration in the early morning was previously thought to be related to strong

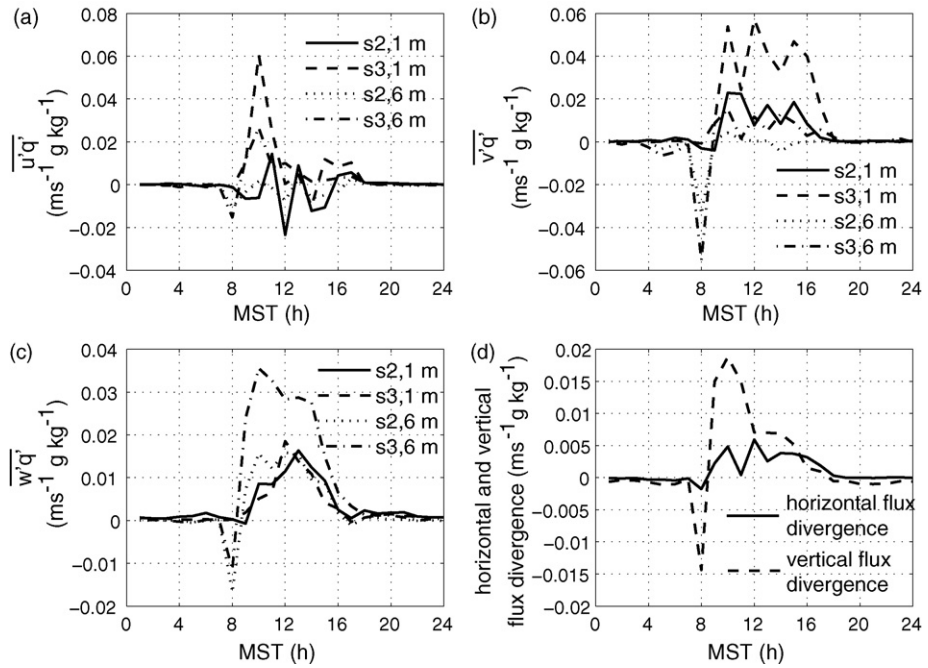

Fig. 13. The diurnal variation of the horizontal and vertical turbulent water vapor fluxes at 1 and 6 m (a, b, and c), and (d) a comparison between the vertically integrated horizontal turbulent water vapor flux divergence $(\int_{1m}^{6m}(\partial\overline{u'q'}/\partial x + \partial\overline{v'q'}/\partial y)\,dz)$ and vertical turbulent water vapor flux divergence $(\overline{w'q'}_{6m} - \overline{w'q'}_{1m})$ for 15 September. Here all the variables are in box coordinates.

venting (Yang et al., 1999). We investigate physical processes which are responsible for morning CO_2 reduction and evening increase for the day of 15 September. Before the large CO_2 drop, there was a period of upward CO_2 and water vapor turbulent transport between 4 and 6 MST (Fig. 14 d and f). However, at that time, the sun was not up yet (Fig. 14c). The upward CO_2 and water vapor fluxes were generated by the arrival of a wind gust (Fig. 14b), which also warmed the layer adjacent to the canopy top. Due to the stable boundary layer, the magnitudes of the upward CO_2 and water vapor turbulent fluxes were relatively small and the CO_2 and water vapor mixing ratios did not decrease significantly around 7 MST. As the wind switched direction from downslope to upslope (Fig. 14a), the nighttime accumulated moist and CO_2-rich air was brought up by the upslope flow, leading to a surge of water vapor throughout the canopy layer (Fig. 14e), but not CO_2 (Fig. 14c). By then, there was enough sunlight for photosynthesis, and leaf stomata took in CO_2 but released water vapor. The photosynthesis is observed as downward CO_2 and upward water vapor turbulent fluxes. The CO_2 uptake was also captured by horizontal CO_2 advection as evident in the switch of the horizontal advection from positive to negative in Fig. 10. The temperature signature of the cold, moist, and CO_2-rich pool accumulated at the low ground over the night was not detectable by the time the upslope flow arrived as the ground had already slowly warmed (not shown). The evidence of nighttime accumulated moist CO_2-rich air brought up by the upslope flow in the early morning was also shown in the composite 1-m water vapor and CO_2 concentrations, and the timing of the water vapor surge is also consistent with the composite wind direction switch (not shown). As the canopy continued warming, the canopy at the maximum leaf density level warms up the fastest, leading to an unstable layer above it and a stable layer below between 8 and 9 MST. The unstable layer led to strong convective turbulent mixing, and large downward CO_2 and upward water vapor fluxes as stomata were open by then. The convective mixing led to significant CO_2 and water vapor reduction as they were dispersed into a deeper boundary layer. At the same time, the CO_2 uptake was continually captured by the horizontal CO_2 advection throughout the day until sunset; the stable layer close to the ground can last throughout the day except for several hours around noon.

Close to the sunset, stomata closed and the longwave radiation led to development of a stable boundary layer atop of the canopy, which suppressed CO_2 and water vapor turbulent mixing. Ecosystem respiration led to increasing CO_2 (Fig. 14c), and ground evaporation led

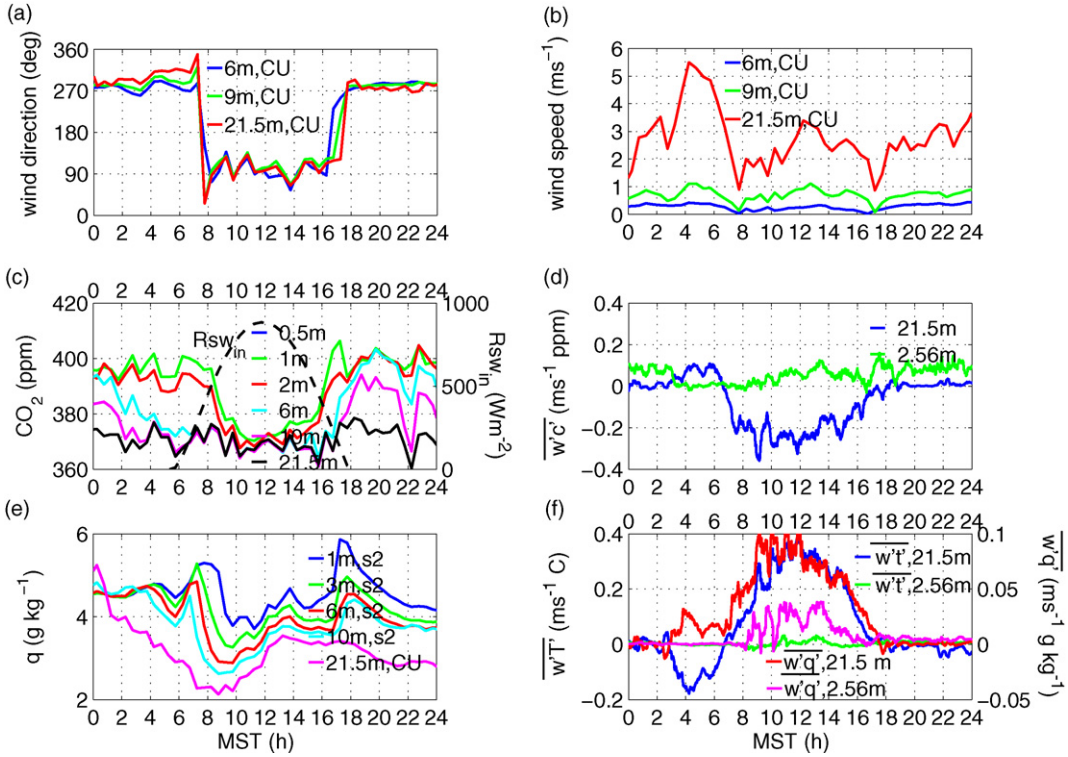

Fig. 14. The diurnal variation of (a) wind direction and (b) wind speed at the CU tower, (c) CO_2 concentration at various heights and the downward solar radiation (Rsw_{in}) at the CU tower, (d) CO_2 fluxes within and above the canopy layer at the CU tower, (e) specific humidity at the CU tower and s2, and (f) heat and water vapor fluxes within and above the canopy layer at the CU tower for 15 September 2002.

to increasing water vapor (Fig. 14e). As the drainage flow developed, the air with relatively low CO_2 and water vapor from high elevation was drained downslope, which replaced the locally respired high CO_2. Thus, the CO_2 advection switched from negative to positive (Fig. 10).

5. Discussions and summary

Three dimensional CO_2 transport over the Niwot Ridge AmeriFlux forest site on a $\sim$5% slope was investigated by supplementing the existing measurements during the NIWOT02. Due to the decoupling between the canopy flow and the overlying prevailing westerly flow, we found a consistent diurnal pattern of downslope flow at night and upslope flow during daytime within the canopy. The drainage flow is sensitive to turbulent mixing and topography. Under weak wind conditions, we observed that drainage flow occurred not only along the overall terrain slope and extended to the top of the canopy layer, but also down a local slope towards a 2-m-wide Creek. The respired CO_2 was drawn towards Como Creek and transported down the creek analogous to water drainage. The spatial variation of CO_2 concentration associated with the creek drainage flow can be eliminated by turbulent mixing generated by shear instability from strong synoptic westerlies. In contrast, the horizontal CO_2 gradient along the main terrain slope can survive turbulent mixing events from above the canopy, resulting in high CO_2 concentration down the area terrain slope. The canopy layer not only protects the drainage flow from being eliminated by turbulence, but also limits the vertical CO_2 transport. We found that the CO_2 concentration was highest when the within-canopy wind was along the drainage-flow direction. The high-CO_2 air was associated with the respired CO_2 capped by a stable boundary layer above the canopy, which is favorable for drainage flow development. In addition, the high CO_2 could also be related to soil respiration induced by pressure perturbations and diffusion.

We investigated the early morning CO_2 reduction in detail for September 15. We observed a period of weak upward CO_2 and water vapor turbulent fluxes and downward heat flux right before sunrise because of a wind gust. Due to the stable boundary layer at the time, the turbulent mixing was weak and the reduction of CO_2 and water vapor within the canopy and above was small.

By the time the upslope flow developed, leaf stomata had already opened as there was enough sunlight. The moist and CO_2-rich air that had accumulated over the night at low elevation was carried upslope, which led to a surge of water vapor but not CO_2 as stomata absorbed CO_2 and released water vapor. The CO_2 uptake was demonstrated not only in the downward CO_2 flux and upward water vapor flux, but also in the horizontal CO_2 advection. As the solar heating continued, the canopy at the maximum leaf area density height warmed up the fastest, leading to unstable convective turbulent mixing above and a stable layer below. The convective turbulent mixing led to the final vanishing of CO_2 and water vapor build-up over the night. In spite of the convective mixing throughout the day, we found that the CO_2 uptake was also detectable in the horizontal CO_2 advection, which was caused by the CO_2 reduction by stomata uptake as the upslope flow passed through the canopy. The upslope transport of nighttime accumulated moist and CO_2-rich air in early morning was often observed at the site as evident in their composite time series.

As we demonstrated in this study, all the CO_2 transport terms are important in estimating NEE, especially over complex terrain. At night, both the vertical CO_2 turbulent flux and the CO_2 storage are negligible compared to either horizontal or vertical CO_2 advection. Drainage flow can remove locally respired CO_2 and replace it with low CO_2 respired at higher elevations. However, the net effect of horizontal and vertical CO_2 advection is complicated by the fact that they can have opposite signs with similar magnitudes at night. Of the two advection terms, vertical CO_2 advection has the largest uncertainty. First, vertical velocities are sensitive to the coordinates used and how well the anemometers are aligned with local gravity. Second, the vertical CO_2 gradient is large at night, and any small errors in vertical velocity could lead to large errors in the estimate of vertical CO_2 advection. During daytime, the vertical CO_2 turbulent transport is much stronger than either advection term. Open stomata can absorb CO_2 regardless of whether flow is generated by orography or synoptic flow. As a result of convective turbulence mixing, the CO_2 reduction along the wind direction is not as significant as at night; however, it is still detectable. The negative horizontal CO_2 advection within the daytime stable sub-canopy layer implies that enough direct and diffuse sunlight penetrated into the CO_2-rich stable layer to trigger photosynthesis. Since the shaded stable layer close to the ground can survive throughout the day and suppress turbulent fluxes, photosynthesis there cannot be monitored solely by vertical CO_2 turbulent flux and time variations of the CO_2 concentration at isolated towers.

Although accurate estimates of NEE_m are difficult, our analysis demonstrated some general characteristics of CO_2 transport over complex terrain. We found that the traditional method of estimating NEE using isolated towers may underestimate both respiration at night and photosynthesis during daytime. Although all the CO_2 transport processes discussed in this study are over complex terrain, the same processes should occur over even seemingly flat terrain since truly flat land with no drainage flow is relatively rare. Both horizontal and vertical advection of CO_2 are subject to any flow passing through forest regardless of whether flow is induced by orographic effects, synoptic flow, or surface heterogeneity as long as turbulent mixing is not strong enough to eliminate the CO_2 gradient. Long-term regional NEE depends on the sum of all the CO_2 budget terms, not just individual terms. Long-term observations of all the CO_2 budget terms are necessary even over ''flat'' terrain.

Acknowledgments

The study was supported by the NCAR opportunity fund, the NCAR Biogeoscience Initiative, and NSF grant EAR-0321918. We would like to thank the staff members of ISFF at NCAR/EOL for their hard work and support to the NIWOT02. The leaf area density data from Dr. Chuixiang Yi are gratefully acknowledged. NCAR is sponsored by the National Science Foundation.

References

Albertson, J.D., Parlange, M.B., 1999. Natural integration of scalar fluxes from complex terrain. Adv. Water Res. 23, 239–252.

Anderson, D.E., Turnipseed, A., Estimating nocturnal respiration from profile measurements in a subalpine forest. EOS Trans., AGU 82 (47), Fall Meet. Suppl. Abstract B41A-12, 2001.

Aubinet, M., Heinesch, B., Yernaux, M., 2003. Horizontal and vertical CO_2 advection in a sloping forest. Boundary-Layer Meteorol. 108, 397–417.

Aubinet, M., Berbigier, P., Bernhofer, Ch., Cescatti, A., Feigenwinter, C., Granier, A., Grünwald, Th., Havrankova, K., Heinesch, B., Longdoz, B., Marcolla, B., Montagnani, L., Sedlak, P., 2005. Comparing CO_2 storage and advection conditions at night at different CARBOEUROFLUX sites. Boundary-Layer Meteorol. 116, 63–94.

Baldocchi, D., Finnigan, J., Wilson, K., Paw, U.K.T., Falge, E., 2000. On measuring net ecosystem carbon exchange over tall vegetation on complex terrain. Boundary-Layer Meteorol. 96, 257–291.

Banta, B.M., Cotton, W.R., 1981. An analysis of the structure of local wind systems in a broad mountain basin. J. Appl. Meteorol. 20 (11), 1255–1266.

Banta, B.M., 1982. An observational and numerical study of mountain boundary-layer flow. Ph.D. Thesis from Department of Atmospheric Science, Colorado State University, Fort Collins, Colorado, Atmospheric Science Paper no. 350.

Banta, B.M., 1984. Daytime boundary-layer evolution over mountainous terrain. Part I: Observations of the dry circulations. Mon. Wea. Rev. 112 (2), 340–356.

Barry, R.G., 1973. A climatological transect on the east slope of the front range, Colorado. Arctic Alpine Res. 5 (2), 89–110.

Bousquet, P., Peylin, P., Ciais, P., Le Quéré, C., Friedlingstein, P., Tans, P.P., 2000. Regional changes in carbon dioxide fluxes of land and oceans since. Science 290, 1342–1346.

Brazel, A.J., Brazel, S.W., 1983. Summer diurnal wind patterns at 3000 m surface level, front range, Colorado, U.S.A. Phys. Geogr. 4 (1), 53–61.

Brost, R.A., Wyngaard, J.C., 1978. A model study of the stably stratified planetary boundary layer. J. Atmos. Soc. 35, 1427–1440.

Burns, S., Sun, J., Oncley, S., Delany, A., Stephens, B., Anderson, D., Schimel, D., Lenschow, D.H., Monson, R., 2006. Measurements of the diurnal cycle of temperature, humidity, wind, and carbon dioxide in a subalpine forest during the carbon in the mountains experiment (CME04). In: Proceedings of the 17th Symposium on Boundary Layers and Turbulence and 27th Conference on Agricultural and Forest Meteorology, San Diego, CA. American Meteorological Society.

Ciais, P., Tans, P.P., Trolier, M., White, J.W.C., Francey, R.J., 1995. A large Northern Hemisphere terrestrial CO_2 sink indicated by the $^{13}C/^{12}C$ ratio of atmospheric CO_2. Science 269, 1098–1102.

Clements, W.E., Archuleta, J.A., Gudiksen, P.H., 1989. Experimental design of the 1984 ASCOT field study. J. Appl. Meteorol. 28, 405–413.

Ellison, T.H., Turner, J.S., 1959. Turbulent entrainment in stratified flows. J. Fluid Mech. 6, 423–448.

Fan, S., Gloor, M., Mahlman, J., Pacala, S., Sarmiento, J., Takahashi, T., Tans, P., 1998. A large terrestrial carbon sink in North America implied by atmospheric and oceanic carbon dioxide data and models. Science 282, 442–446.

Feigenwinter, C., Bernhofer, C., Vogt, R., 2004. The influence of advection on the short-term CO_2-budget in and above a forest canopy. Boundary-Layer Meteorol. 113 (2), 201–224.

Finnigan, J., 1999. A comment on the paper by Lee (1998): on micrometeorological observations of surface-air exchange over all vegetation. Agric. Forest. Meteorol. 97, 55–64.

Finnigan, J., 2000. Turbulence in plant canopies. Annu. Rev. Fluid Mech. 32, 519–571.

Finnigan, J.J., Belcher, S.E., 2004. Flow over a hill covered with a plant canopy. Quart. J. Roy. Meteorol. Soc. 130, 1–29.

Finnigan, J.J., 2004a. Advection and modeling. In: Lee, X., Massman, W., Law, B. (Eds.), Handbook of Micrometeorology—A Guide for Surface Flux Measurement and Analysis. Kluwer Academic Publishers, pp. 209–244.

Finnigan, J., 2004b. The footprint concept in complex terrain. Agric. Forest. Meteorol. 127, 117–129.

Finnigan, J., 2006. The storage term in eddy flux calculations. Agric. Forest. Meteorol. 136, 108–113.

Froelich, N.J., Schmid, H.P., Grimmond, C.S.B., Su, H.-B., Oliphant, A.J., 2005. Flow divergence and density flows above and below a deciduous forest. Part I. Non-zero mean vertical wind above canopy. Agric. Forest. Meteorol. 133, 140–152.

Froelich, N.J., Schmid, H.P., 2006. Flow divergence and density flows above and below a deciduous forest. Part II. Below-canopy thermotopographic flows. Agric. Forest. Meteorol. 138, 29–43.

Geiger, R., Aron, R.H., Todhunter, P., 1995. The Climate Near the Ground. Vieweg, p. 528.

Glinski, J., Stepniewski, W., 1985. Soil Aeration and its Role for Plants. CRC Press, Boca Raton, FL.

Goulden, M.L., Munger, J.W., Fan, S.M., Daube, B.C., Wofsy, S.C., 1996. Measurements of carbon sequestration by long-term eddy covariance: methods and a critical evaluation of accuracy. Global Change Biol. 2, 169–182.

Helmis, C.G., Asimakopoulos, D.N., Deligiorgi, D.G., Petrakis, M.C., 1990. Some observations on the destruction of morning temperature inversions in a large and broad mountain valley. J. Appl. Meteorol. 29, 396–400.

Horst, T.W., Doran, J.C., 1986. Nocturnal drainage flow on simple slopes. Boundary-Layer Meteorol. 34, 263–286.

Howell, J.F., Mahrt, L., 1997. Multiresolution flux decomposition. Boundary-Layer Meteorol. 83, 117–137.

Hunt, J.C.R., Fernando, H.J.S., Princevac, M., 2003. Unsteady thermally driven flows on gentle slopes. J. Atmos. Soc. 60, 2169–2182.

Jarvis, P.G., Massheder, J.M., Hale, S.E., Moncrieff, J.B., Rayment, M., Scott, S.L., 1997. Seasonal variation of carbon dioxide, water vapor, and energy exchanges of a boreal black spruce forest. J. Geophys. Res. 102, 28953–28966.

Kaimal, J.C., Finnigan, J.J., 1994. Atmospheric Boundary Layer Flows—their Structure and Measurement. Oxford University Press, 289 pp.

Katul, G.G., Finnigan, J.J., Poggi, D., Leuning, R., Belcher, S.E., 2006. The influence of hilly terrain on canopy-atmosphere carbon dioxide exchange. Boundary-Layer Meteorol. 118, 189–216.

Kimball, B.A., Lemon, E.R., 1971. Air turbulence effects upon soil gas exchange. Soil Sci. Soc. Am. Proc. 35, 16–21.

King, C.W., 1997. A climatology of thermally forced circulations in oppositely oriented airsheds along the continental divide in Colorado. NOAA Technical Memorandum ERL ETL-283. p. 152.

Kominami, Y., Miyama, T., Tamai, K., Nobuhiro, T., Goto, Y., 2003. Characteristics of CO_2 flux over a forest on complex topography. Tellus 55B, 313–321.

Kondo, J., Sato, T., 1988. A simple model of drainage flow on a slope. Boundary-Layer Meteorol. 43, 103–123.

Kondo, J., Kuwagata, T., Haginoya, S., 1989. Heat budget analysis of nocturnal cooling and daytime heating in a basin. J. Atmos. Soc. 46, 2917–2933.

Kossmann, M., Vögtlin, R., Corsmeier, U., Vogel, B., Fiedler, F., Binder, H.-J., Kalthoff, N., Beyrich, F., 1998. Aspects of the convective boundary layer structure over complex terrain. Atmos. Environ. 32 (7), 1323–1348.

Kuwagata, T., Kondo, J., 1989. Observation and modeling of thermally induced upslope flow. Boundary-Layer Meteorol. 49, 265–293.

Lee, X., 1998. On micrometeorological observations of surface-air exchange over tall vegetation. Agric. Forest. Meteorol. 91, 39–49.

Lee, X., Hu, X., 2002. Forest-air fluxes of carbon, water and energy over non-flat terrain. Boundary-Layer Meteorol. 103, 277–301.

Lee, X., 2004. Forest-air exchange in non-ideal conditions: the role of horizontal flux and its divergence. In: Grace, J., Moncrieff, J., McNaughton, K.G. (Eds.), Forests at the Land-Atmosphere Interface. CAB International, pp. 145–157.

Leuning, R., 2004. Measurements of trace gas fluxes in the atmosphere using eddy covariance: WPL corrections revisited. In: Lee, X., Massman, W., Law, B. (Eds.), Handbook of Micrometeorology—A Guide for Surface Flux Measurement and Analysis. Kluwer Academic Publishers, pp. 119–132.

Mahrt, L., Larsen, S., 1990. Relation of slope wind to the ambient flow over gentle terrain. Boundary-Layer Meteorol. 53, 93–102.

Mahrt, L., Vickers, D., Nakamura, R., Soler, M.R., Sun, J., Burns, S., Lenschow, D.H., 2001. Shallow drainage flows. Boundary-Layer Meteorol. 101, 243–260.

Marcolla, B., Cescatti, A., Montagnani, L., Manca, G., Kerschbaumer, G., Minerbi, S., 2005. Importance of advection in the atmospheric CO_2 exchanges of an alpine forest. Agric. Forest. Meteorol. 130, 193–206.

May, P.T., Wilczak, J.M., 1993. Diurnal and seasonal variations of boundary-layer structure observed with a radar profiler and RASS. Mon. Wea. Rev. 121, 673–682.

McKee, T.B., O'Neal, R.D., 1989. The role of valley geometry and energy budget in the formation of nocturnal valley winds. J. Appl. Meteorol. 28, 445–456.

Monson, R.K., Turnipseed, A.A., Sparks, J.P., Harley, P.C., Scott-Denton, L.E., Sparks, K., Huxman, T.E., 2002. Carbon sequestration in a high-elevation, subalpine forest. Global Change Biol. 8, 459–478.

Monson, R.K., Lipson, D.L., Burns, S.P., Turnipseed, A.A., Delany, A.C., Williams, M.W., Schmidt, S.K., 2006. Winter forest soil respiration controlled by climate and microbial community composition. Nature 439, 711–714.

Moren, A.-S., Lindroth, A., 2000. CO_2 exchange at the floor of a boreal forest. Agric. Forest. Met. 101, 1–14.

Nakane, K., 1975. Dynamics of soil organic matter in different parts on a slope under evergreen oak forest. Jpn. J. Ecol. 25 (4), 206–216.

Orgill, M.M., Schreck, R.I., 1985. An overview of the ASCOT multi-laboratory field experiments in relation to drainage winds and ambient flow. Bull. Am. Meteorol. Soc. 66, 1263–1277.

Parrish, D.D., Hahn, C.H., Fahey, D.W., Williams, E.J., Bollinger, M.J., Hübler, G., Buhr, M.P., Murphy, P.C., Trainer, M., Hsie, E.Y., Liu, S.C., Fehsenfeld, F.C., 1990. Systematic variations in the concentration of NO_x (NO plus NO_2) at Niwot Ridge, Colorado. J. Geophys. Res. 95 (D2), 1817–1836.

Rao, K.S., Tangirala, R.S., Hosker Jr., R.P., 1991. Tracer distributions in Brush Creek Valley drainage flow derived from 1984 ASCOT data. NOAA Technical Memorandum ERL ARL-191, p. 55.

Schimel, D., Kittel, T.G.F., Running, S., Monson, R., Turnipseed, A., Anderson, D., 2002. Carbon sequestration studied in Western U.S. mountains. EOS 83 (40), 445–449.

Schmid, H.P., 2002. Footprint modeling for vegetation atmosphere exchange studies: a review and perspective. Agric. Forest. Meteorol. 113, 159–183.

Scott-Denton, L.E., Sparks, K.L., Monson, R.K., 2003. Spatial and temporal controls of soil respiration rate in a high-elevation, subalpine forest. Soil Biol. Biochem. 35, 525–534.

Shaw, R.H., 1977. Secondary wind speed maxima inside plant canopies. J. Appl. Meteorol. 16, 514–521.

Staebler, R.M., 2003. Forest subcanopy flows and micro-scale advection of carbon dioxide. PhD dissertation, the University at Albany, State University of New York, College of Arts and Sciences, Department of Earth and Atmospheric Sciences.

Staebler, R.M., Fitzjarrald, D.R., 2004. Observing subcanopy CO_2 advection. Agric. Forest. Meteorol. 122, 139–156.

Sun, J., Mahrt, L., 1995. Relationship of the heat flux to microscale temperature variations: application to BOREAS. Boundary-Layer Meteorol. 76, 291–301.

Sun, J., Esbensen, S.K., Mahrt, L., 1995. Estimation of surface heat flux. J. Atmos. Soc. 52, 3162–3171.

Sun, J., Desjardins, R., Mahrt, L., MacPherson, I., 1998. Transport of carbon dioxide, water vapor, and ozone by turbulence and local circulations. J. Geophys. Res. 103, 25873–25885.

Sun, J., 2007. Tilt corrections over complex terrain and their implication for CO_2 transport. Boundary-Layer Meteorol., in press.

Tans, P.P., Fung, I.Y., Takahashi, T., 1990. Observational constraints on the global atmospheric CO_2 budget. Science 247, 1431–1438.

Toth, J.J., Johnson, R.H., 1985. Summer surface flow characteristics over Northeast Colorado. Mon. Wea. Rev. 113, 1458–1469.

Turnipseed, A.A., Blanken, P.D., Anderson, D.E., Monson, R.K., 2002. Energy budget above a high-elevation subalpine forest in complex terrain. Agric. Forest. Meteorol. 110, 177–201.

Turnipseed, A.A., Anderson, D.E., Blanken, P.D., Baugh, W.M., Monson, R.K., 2003. Airflows and turbulent flux measurements in mountainous terrain. Part I. Canopy and local effects. Agric. Forest. Meteorol. 119, 1–21.

Turnipseed, A.A., Anderson, D.E., Burns, S., Blanken, P.D., Monson, R.K., 2004. Airflows and turbulent flux measurements in mountainous terrain Part 2: Mesoscale effects. Agric. Forest. Meteorol. 125, 187–205.

Van Gorsel, E., Christen, A., Feigenwinter, C., Parlow, E., Vogt, R., 2003. Daytime turbulence statistics above a steep forested slope. Boundary-Layer Meteorol. 109, 311–329.

Veblen, T.T., 1986. Age and size structure of subalpine forests in the Colorado front range. Bull. Torrey Bot. Club 113 (3), 225–240.

Vickers, D., Mahrt, L., 2003. The cospectral gap and turbulent flux calculations. J. Atmos. Oceanic Tech. 20 (5), 660–672.

Vickers, D., Mahrt, L., 2006. A solution for flux contamination by mesoscale motions with very weak turbulence. Boundary-Layer Meteorol. 118, 431–447.

Wang, W., Davis, K.J., Cook, B.D., Bakwin, P.S., Yi, C., Butler, M.P., Ricciuto, D.M., 2005. Surface layer CO_2 budget and advective contributions to measurements of net ecosystem-atmosphere exchange of CO_2. Agric. Forest. Meteorol. 135, 202–214.

Whiteman, C.D., 2000. Mountain Meteorology: Fundamentals and Applications. Oxford University Press.

Witkamp, M., 1969. Cycles of temperature and carbon dioxide evolution from litter and soil. Ecology 50 (5), 922–924.

Wofsy, S.C., Harris, R.C., Kaplan, W.A., 1988. Carbon dioxide in the atmosphere over the Amazon Basin. J. Geophys. Res. 93, 1377–1387.

Wyngaard, J.C., 2004. Changing the face of small-scale meteorology. In: Fedorovich, E., Rotunno, R., Stevens, B. (Eds.), Atmospheric Turbulence and Mesoscale Meteorology.

Xu, L.-K., Matista, A.A., Hsiao, T.C., 1999. A technique for measuring CO_2 and water vapor profiles within and above plant canopies over short periods. Agric. Forest. Meteorol. 94, 1–12.

Yang, P.C., Black, T.A., Neumann, H.H., Novak, M.D., Blanken, P.D., 1999. Spatial and temporal variability of CO_2 concentration and flux in a boreal aspen forest. J. Geophys. Res. 104 (D22), 27653–27661.

Yi, C., Davis, K.J., Bakwin, P.S., Berger, B.W., Marr, L.C., 2000. Influence of advection on measurements of the net ecosystem-atmosphere exchange of CO_2 from a very tall tower. J. Geophys. Res. 105, 9991–9999.

Yi, C., Monson, R.K., Zhai, Z., Anderson, D.E., Lamb, B., Allwine, G., Turnipseed, A.A., Burns, S.P., 2005. Modeling and measuring the nocturnal drainage flow in a high-elevation, subalpine forest ecosystem with complex terrain. J. Geophys. Res. 110, D22303.